ARTICLE

https://doi.org/10.1038/s41586-019-1111-9

Mapping the world's free-flowing rivers

G. Grill[1]*, B. Lehner[1]*, M. Thieme[2], B. Geenen[3], D. Tickner[4], F. Antonelli[5], S. Babu[6], P. Borrelli[7,8], L. Cheng[9], H. Crochetiere[10], H. Ehalt Macedo[1], R. Filgueiras[11,36], M. Goichot[12], J. Higgins[13], Z. Hogan[14], B. Lip[15], M. E. McClain[16,17], J. Meng[18,19], M. Mulligan[20], C. Nilsson[21,22], J. D. Olden[23], J. J. Opperman[2], P. Petry[24,25], C. Reidy Liermann[26], L. Sáenz[27,28], S. Salinas-Rodríguez[29], P. Schelle[30], R. J. P. Schmitt[31], J. Snider[10], F. Tan[1], K. Tockner[32,33,37], P. H. Valdujo[34], A. van Soesbergen[20] & C. Zarfl[35]

Free-flowing rivers (FFRs) support diverse, complex and dynamic ecosystems globally, providing important societal and economic services. Infrastructure development threatens the ecosystem processes, biodiversity and services that these rivers support. Here we assess the connectivity status of 12 million kilometres of rivers globally and identify those that remain free-flowing in their entire length. Only 37 per cent of rivers longer than 1,000 kilometres remain free-flowing over their entire length and 23 per cent flow uninterrupted to the ocean. Very long FFRs are largely restricted to remote regions of the Arctic and of the Amazon and Congo basins. In densely populated areas only few very long rivers remain free-flowing, such as the Irrawaddy and Salween. Dams and reservoirs and their up- and downstream propagation of fragmentation and flow regulation are the leading contributors to the loss of river connectivity. By applying a new method to quantify riverine connectivity and map FFRs, we provide a foundation for concerted global and national strategies to maintain or restore them.

Rivers are essential sources of environmental health, economic wealth and human well-being. For millennia, rivers have provided food, contributed water for domestic use and agriculture, sustained transportation corridors and, more recently, enabled power generation and industrial production[1]. These goods and services generally require built infrastructure, and society has addressed this demand by constructing an estimated 2.8 million dams (with reservoir areas $>10^3$ m^2)[2], regulating and creating over 500,000 km of rivers and canals for navigation and transport[3,4] and building irrigation and water-diversion schemes. As a result, rivers are exposed to sustained pressure from fragmentation and loss of river connectivity, constraining their capacity to flow unimpeded, affecting many fundamental processes and functions characteristic of healthy rivers[5] and leading to the rapid decline of biodiversity and essential ecosystem services[6].

The capacity of rivers to flow freely is governed by the connectivity of pathways that enable the movement and exchange of water and of the organisms, sediments, organic matter, nutrients and energy that it conveys throughout the riverine environment. River connectivity extends in four dimensions: longitudinally (up- and downstream in the river channel), laterally (between the main channel, the floodplain and riparian areas), vertically (between the groundwater, the river and the atmosphere) and temporally (seasonality of flows)[7,8]. River connectivity is also spatially and temporally dynamic, largely driven by the natural flow regime[9], enabling and regulating hydrological, geomorphic and ecological processes in river networks and providing the aquatic medium for matter and species to move along the river and into adjacent habitats[10]. Humans have altered natural river connectivity in multiple ways, either directly, by placing structures into the longitudinal or lateral flow paths, such as dams and levees, or indirectly, by altering the hydrological, thermal and sediment regimes of the river[11,12].

Although it is inherently complex to quantify the value of services provided by FFRs or to measure the devaluing effect of impeding infrastructure, many examples exist that underline the importance of connectivity for the provision of natural riverine ecosystem functions and processes. For instance, floodplains are among the most productive and diverse riverine ecosystems globally[13], and their disconnection from the upstream catchment or river channel alters ecosystem services such as natural flood storage, nutrient retention and flood–recession agriculture[14]. Built river infrastructure has also been linked to declines in terrestrial and freshwater species[11,15–17], and sediment capture by dams may cause the alteration of the geomorphic dynamics of rivers and the shrinking of river deltas worldwide[18]. Although advances in the socio-economic valuation of river connectivity have emerged—for example, inland fisheries provide the equivalent of all dietary animal protein for 158 million people globally, particularly for poor and undernourished populations[19]—more comprehensive and detailed studies are needed[20].

Acknowledging the importance of river connectivity, a decade ago the Brisbane Declaration[21] called for the identification and conservation of "a global network of FFRs", and in 2015 the world's governments committed to "protect and restore water-related ecosystems" under the United Nations' Sustainable Development Goals (target 6.6). Nevertheless, continued and accelerating declines in river connectivity, aquatic biodiversity and associated ecosystem services remain a

[1]Department of Geography, McGill University, Montreal, Québec, Canada. [2]WWF-US, Washington, DC, USA. [3]WWF-NL, Zeist, The Netherlands. [4]WWF-UK, Woking, UK. [5]WWF-Mediterranean, Rome, Italy. [6]WWF-India, New Delhi, India. [7]Environmental Geosciences, University of Basel, Basel, Switzerland. [8]European Commission, Joint Research Centre, Directorate for Sustainable Resources, Ispra, Italy. [9]WWF-China, Beijing, China. [10]WWF-Canada, Toronto, Ontario, Canada. [11]WWF-Zambia, Lusaka, Zambia. [12]WWF Greater Mekong Programme, Ho Chi Minh City, Vietnam. [13]The Nature Conservancy (TNC), Chicago, IL, USA. [14]Department of Biology and Global Water Center, University of Nevada, Reno, NV, USA. [15]WWF-Malaysia, Sarawak, Malaysia. [16]Department of Water Science and Engineering, IHE Delft, Delft, The Netherlands. [17]Department of Water Management, Delft University of Technology, Delft, The Netherlands. [18]WWF-Germany, Berlin, Germany. [19]HTWG Konstanz University of Applied Sciences, Konstanz, Germany. [20]Department of Geography, King's College London, London, UK. [21]Department of Ecology and Environmental Science, Umeå University, Umeå, Sweden. [22]Department of Wildlife, Fish and Environmental Studies, Swedish University of Agricultural Sciences, Umeå, Sweden. [23]School of Aquatic and Fishery Sciences, University of Washington, Seattle, WA, USA. [24]The Nature Conservancy, Hollis, NH, USA. [25]Museum of Comparative Zoology, Harvard University, Cambridge, MA, USA. [26]UW Center for Limnology, University of Wisconsin-Madison, Madison, WI, USA. [27]Conservation International (CI), Arlington, VA, USA. [28]Environmental Engineering, Michigan Technological University (MTU), Houghton, MI, USA. [29]WWF-Mexico, Mexico City, Mexico. [30]WWF International, Gland, Switzerland. [31]Natural Capital Project, Department of Biology and the Woods Institute for the Environment, Stanford University, Stanford, CA, USA. [32]Leibniz-Institute of Freshwater Ecology and Inland Fisheries (IGB), Berlin, Germany. [33]Institute of Biology, Freie Universität Berlin, Berlin, Germany. [34]WWF-Brazil, Brasília, Brazil. [35]Center for Applied Geoscience, Eberhard Karls University of Tübingen, Tübingen, Germany. [36]Present address: Rewilding Europe, Nijmegen, The Netherlands. [37]Present address: Austrian Science Fund, FWF, Vienna, Austria. *e-mail: guenther.grill@mail.mcgill.ca; bernhard.lehner@mcgill.ca

global challenge. The rising demands for energy, water supply and flood management increasingly call for engineering solutions such as the construction of dams, levees and other water-diversion structures. Indeed, more than 3,700 hydropower dams (>1 MW) are currently planned or under construction worldwide[22]. Asia is a hotspot for dam construction with over 15 GW capacity added in 2016, and the Balkans, the Amazon, China and the Himalayas are facing major booms in hydropower construction[23,24]. Furthermore, several countries are either planning or building extensive inland water-transfer and navigation schemes (for example, India, China and Brazil), which require river dredging, channelization or the instalment of locks and dams[25].

Paramount to the conservation and restoration of FFRs is the availability of a comprehensive global information system that allows assessing the current state and monitoring future trends of river connectivity. Previously, fragmentation and flow regulation by dams were either quantified worldwide at relatively coarse spatial scales[26,27] providing snapshot assessments for large river basins only[28], or relied on spatially inexplicit surrogates for dam impact, such as dam density[17]. Recent improvements in the accessibility and resolution of global hydrological data have allowed more detailed and comprehensive assessments of rivers, including the development of advanced metrics of fragmentation at the river-reach scale[29]. Building on these advances, we provide the first high-resolution and replicable global assessment of the location and extent of FFRs.

Without an existing scientific definition of FFRs, practitioners and scholars have in the past used the term 'free-flowing' to describe rivers that are 'unimpounded' or 'unregulated' by the presence of dams or by flow alterations downstream of reservoirs[27,28,30]. Expanding on this traditional view, which focused mostly on longitudinal connectivity, we here propose a more comprehensive definition based on four dimensions of connectivity, explicitly recognizing that connectivity is necessary within all of those dimensions for a river to flow freely.

We define FFRs as rivers where ecosystem functions and services are largely unaffected by changes to the fluvial connectivity, allowing unobstructed movement and exchange of water, energy, material and species within the river system and with surrounding landscapes. Fluvial connectivity encompasses longitudinal (river channel), lateral (floodplains), vertical (groundwater and atmosphere) and temporal (intermittency) components (Box 1) and can be compromised by (i) physical infrastructure in the river channel, along riparian zones or in adjacent floodplains; (ii) hydrological alterations of river flow due to water abstractions or regulation; and (iii) changes to water quality that lead to ecological barrier effects caused by pollution or alterations in water temperature.

Following this definition, we identified five pressure factors to represent the main human interferences within the four dimensions of fluvial or river connectivity: (1) river fragmentation (longitudinal); (2) flow regulation (lateral and temporal); (3) sediment trapping (longitudinal, lateral and vertical); (4) water consumption (lateral, vertical and temporal); and (5) infrastructure development in riparian areas and floodplains (lateral and longitudinal). There are additional pressures that would merit inclusion, such as temperature alterations, changes in hyporheic flows under and alongside rivers, and pollution. However, owing to the lack of suitable datasets at the global scale, we are unable to include them in this assessment.

To quantify each of the five pressure factors, we compiled and constructed six representative proxies, that is, pressure indicators, informed by available global data and numerical model outputs (Extended Data Table 1). The analyses were conducted using a high-resolution (500 m) river network model[31] that comprises about 8.5 million individual river reaches, with an average reach length of 4.2 km. For the purpose of this paper, we define a 'river reach' as a cartographic—rather than a functional—unit, represented by the smallest spatial element of our river network, that is, the line segment between two neighbouring confluences; a 'river stretch' as two or more contiguous reaches, but not the entire river; and a 'river' as the aggregation of river reaches that form a single-threaded, contiguous flow path from the headwater source to the river outlet (that is, the river's mouth at the ocean, an inland depression or a confluence with a larger river). Guided by published literature and expert judgement, we applied a set of weights within a multi-criteria model to derive a novel, integrated connectivity status index (CSI) that quantifies connectivity ranging from 0% to 100%, which was applied to every individual river reach. Finally, we defined FFRs as those rivers with a CSI at or above 95% over their entire length from source to river outlet (Box 1) and then mapped their distribution and quantified their extent.

Box 1

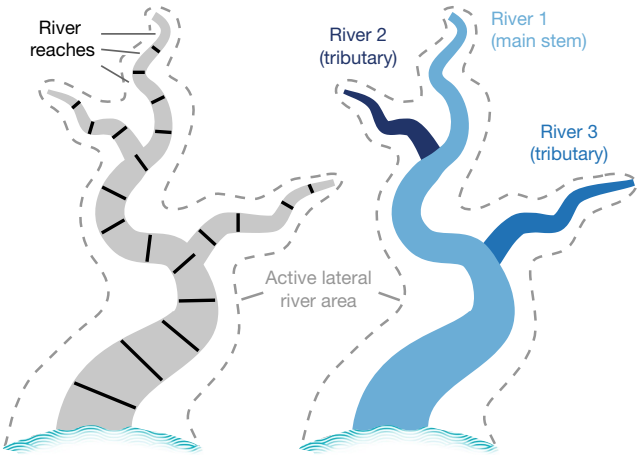
Hydrographic framework and definition of free-flowing rivers

We propose a definition of free-flowing rivers (FFRs) that expands beyond previous efforts and is based on five pressure factors that relate to four connectivity dimensions. Our methodology uses global datasets of hydrography and pressure indicators to create an integrated connectivity status index (CSI). Only rivers with high levels of connectivity in their entire length are classified as free-flowing. For further details see Extended Data Figs. 1, 2.

Hydrographic framework. River reach: smallest element in the river network and unit for the calculation of the CSI. River: linear feature that consists of multiple river reaches. Tributaries form new rivers. Free-flowing status is determined at the scale of the entire river.

Connectivity dimensions. Four dimensions are considered to determine the CSI of river reaches: (1) longitudinal (connectivity between up- and downstream), (2) lateral (connectivity to floodplain and riparian areas), (3) vertical (connectivity to groundwater and atmosphere) and (4) temporal (connectivity based on seasonality of flows).

FFR status. Free-flowing river status is determined on the basis of CSI. Only rivers with high levels of connectivity (CSI $\geq$ 95%) throughout their entire length are considered FFRs.



Global river connectivity at river-reach scale

About half of all river reaches globally show diminished connectivity (CSI < 100%; Fig. 1), and almost 10% of analysed global river reaches (more than 1.1 million kilometres) have a CSI value below 95%, indicating major losses of connectivity. Large contiguous river networks with intact natural connectivity (CSI = 100%) remain only in remote regions of the Arctic, in the Amazon Basin and, to a lesser degree, in the Congo Basin.

Dams and reservoirs and their up- and downstream propagation of fragmentation and flow regulation are the leading contributors to major connectivity loss in global river reaches (Fig. 2). The fragmentation effect of dams is the dominant pressure factor in more than two-thirds

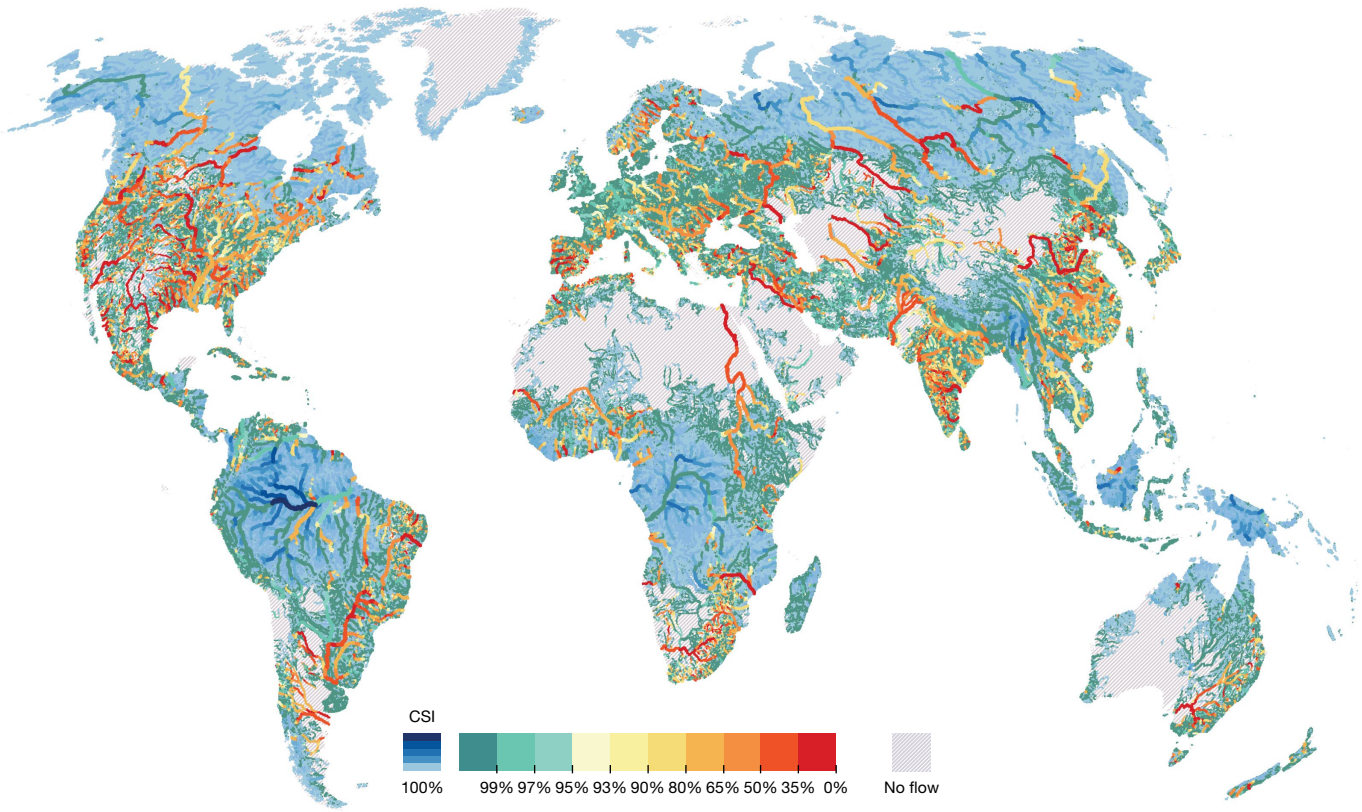


Fig. 1 | Connectivity status index of the world's river reaches. Of all river reaches in the database, 48.2% (by number) are impaired by diminished river connectivity to various degrees (CSI < 100%). The blue shades represent the magnitude of river discharge for river reaches with CSI = 100% (that is, darker shades for larger rivers).

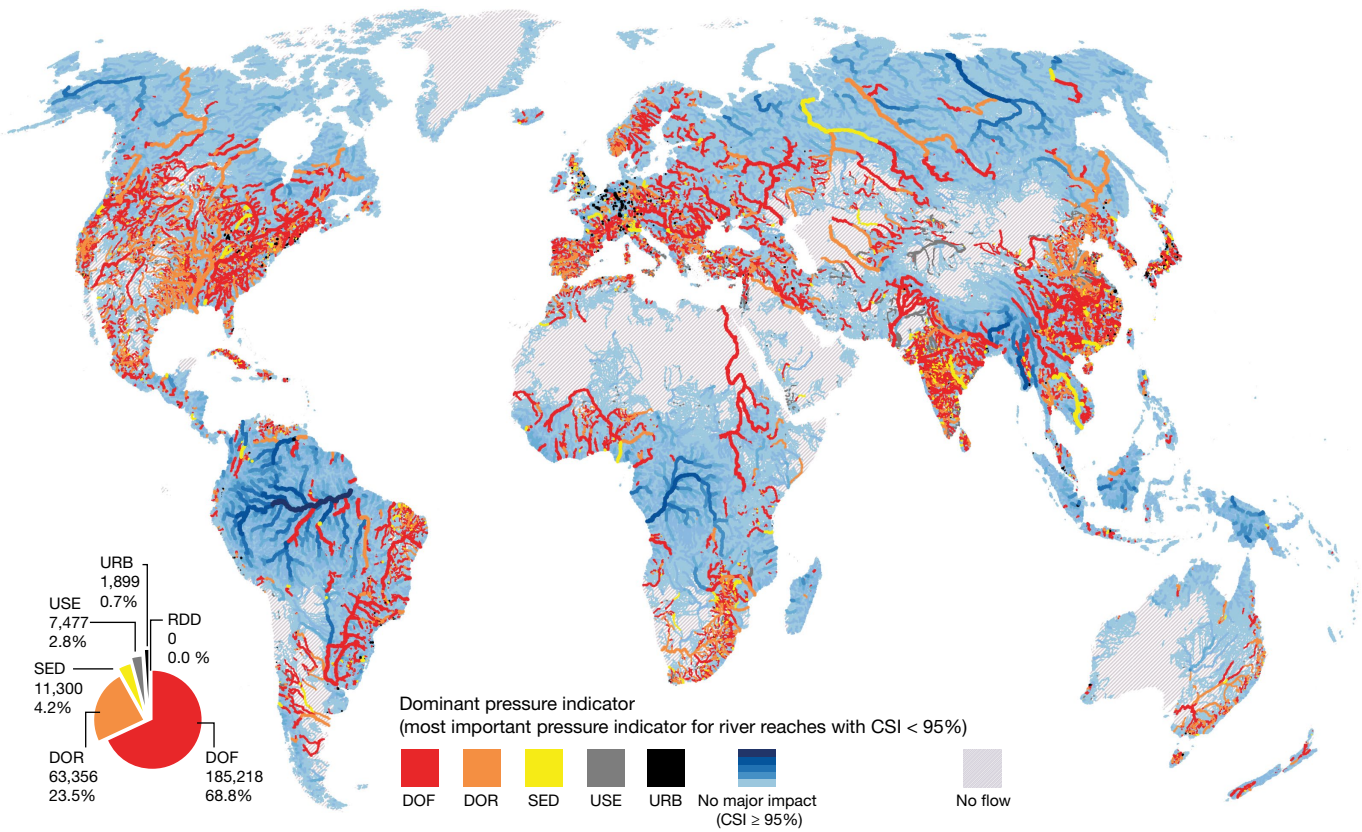


Fig. 2 | Dominant pressure indicator for global river reaches below the CSI threshold of 95%. The dominant pressure indicator—the most important pressure indicator for river reaches with CSI < 95%—contributed the most to the final CSI value after applying the weighting scheme. Pressure indicators include the DOF (degree of fragmentation), DOR (degree of regulation), SED (sediment trapping), USE (consumptive water use) and URB (urban areas). The RDD (road density) does not occur as a dominant pressure indicator on the map. The inset shows the number and proportion of river reaches per dominant pressure indicator at the global scale.

Table 1 | Number and length of the world's free-flowing rivers (FFRs) and non-free-flowing rivers (NFFRs)

	Short (10–100 km)		Medium (100–500 km)		Long (500–1,000 km)		Very long (>1,000 km)		Total
Continent	FFRs	NFFRs	FFRs	NFFRs	FFRs	NFFRs	FFRs	NFFRs	
Number of FFRs and NFFRs									
Africa	34,402	440	2,663	369	129	51	27	31	38,112
Asia	68,472	4,676	3,246	958	113	90	23	46	77,624
Australia	26,889	273	1,045	117	40	20	3	2	28,389
Europe	25,882	1,639	1,344	699	33	66	3	22	29,688
North America	46,504	1,674	2,325	725	43	83	11	33	51,398
South America	78,556	1,234	2,410	414	95	50	23	22	82,804
Total	280,705	9,936	13,032	3,282	453	360	90	156	308,015
% of category	97	3	80	20	56	44	37	63	
Accumulated length ($\times 10^3$ km) of FFRs and NFFRs									
Africa	1,028.2	22.4	468.4	80.0	83.4	34.1	42.1	52.0	1,810.6
Asia	1,900.6	166.1	556.2	188.0	74.4	62.1	41.7	100.0	3,089.1
Australia	629.6	11.3	177.7	23.8	28.3	14.1	4.9	4.3	893.9
Europe	809.0	74.7	221.0	140.8	20.6	47.1	4.4	37.4	1,354.9
North America	1,364.1	72.7	376.9	145.6	28.9	55.8	14.3	62.0	2,120.2
South America	1,837.7	47.6	413.8	86.1	61.8	34.4	40.2	42.8	2,564.4
Total	7,569.1	394.8	2,214.0	664.3	297.3	247.5	147.7	298.4	11,833.1
% of category	95	5	77	23	55	45	33	67	
Number of FFRs and NFFRs connected to the ocean									
Africa	851	37	244	60	16	19	3	14	1,244
Asia	3,355	477	281	172	18	16	8	18	4,345
Australia	5,447	73	345	53	27	9	1	1	5,956
Europe	2,962	323	207	181	9	28	2	14	3,726
North America	5,122	87	462	56	19	29	6	12	5,793
South America	2,468	146	283	118	15	20	1	11	3,062
Total	20,205	1,143	1,822	640	104	121	21	70	24,126
% of category	95	5	74	26	46	54	23	77	

of impacted river reaches below the 95% threshold, followed by flow regulation, affecting one quarter, and sediment trapping, affecting almost 5% of river reaches. Consumptive water use and infrastructure development in riparian areas and floodplains, including roads, urbanization and levees, are important in rivers where dams are less widespread—for example, in highly irrigated regions of India and China—and in densely urbanized areas in western Europe. These pressure factors affect less than 5% of impacted river reaches combined.

Remaining FFRs

By number, 63% of the world's very long rivers (>1,000 km) are no longer free-flowing (Table 1), representing 41% of the global river volume[26]. Both very long and long FFRs (>500 km) are largely absent from the mainland United States, Mexico, Europe and the Middle East, as well as parts of India, southern Africa, southern South America, China and much of Southeast Asia and southern Australia (Fig. 3). The remaining very long and long FFRs are restricted to the northern parts of North America and Eurasia, the Amazon and Orinoco basins in South America, the Congo Basin in Africa and to only a few areas in Southeast Asia, including the Irrawaddy and Salween basins. For example, eight of the ten longest FFRs in South America are located within the Amazon Basin (Supplementary Table 1).

FFRs still connected to the ocean exhibit similar patterns; those that remain are found predominantly in the Arctic, in a few areas in Southeast Asia and in the neo- and afrotropics. Source-to-sea connections have been severed in 77% of very long rivers (>1,000 km) and in 54% of long rivers (500–1,000 km).

Within rivers that are classified as non-free-flowing owing to one or more impacted reaches (CSI < 95%) along their course, there can be extensive stretches that maintain high levels of connectivity. Among non-FFRs worldwide, a total of 542,000 km of river reaches can be classified as having a 'good connectivity status' (CSI ≥ 95%), with 98 contiguous river stretches longer than 500 km, including substantial parts of the Brahmaputra (India and Bangladesh), Orinoco (Venezuela and Colombia) and Amur (Russia) (Fig. 3, Extended Data Table 2).

Validation, limitations and scalability

Our global results suggest that the degree of river connectivity increases with decreasing river length. A total of 56%, 80% and 97% of rivers with lengths of 500–1,000 km, 100–500 km and 10–100 km, respectively, are identified as free-flowing (Table 1). This pattern can be partially attributed to the biased global distribution of small rivers that occur preferentially in the remote, water-rich and relatively unaffected regions of the Amazon and Congo basins. However, it is also important to carefully interpret the status of short rivers, recognizing the limitations of underpinning global datasets in representing pressure factors, particularly the lack of georeferenced data on small dams, barriers and diversions. Our study considers more than 20,000 dams, as provided by global databases[2,32]; yet countless small dams exist worldwide[33]. Therefore, we expect that numerous short rivers are false positives and are classified as free-flowing despite impeding infrastructure projects that are not currently included in global datasets, such as in highly developed regions of Europe and North America. This fundamental data limitation underscores the need for governments and global institutions to fund the acquisition of high-resolution geographic water infrastructure data.

To further corroborate the applied weightings and thresholds, we performed scenario analyses and conducted benchmarking and

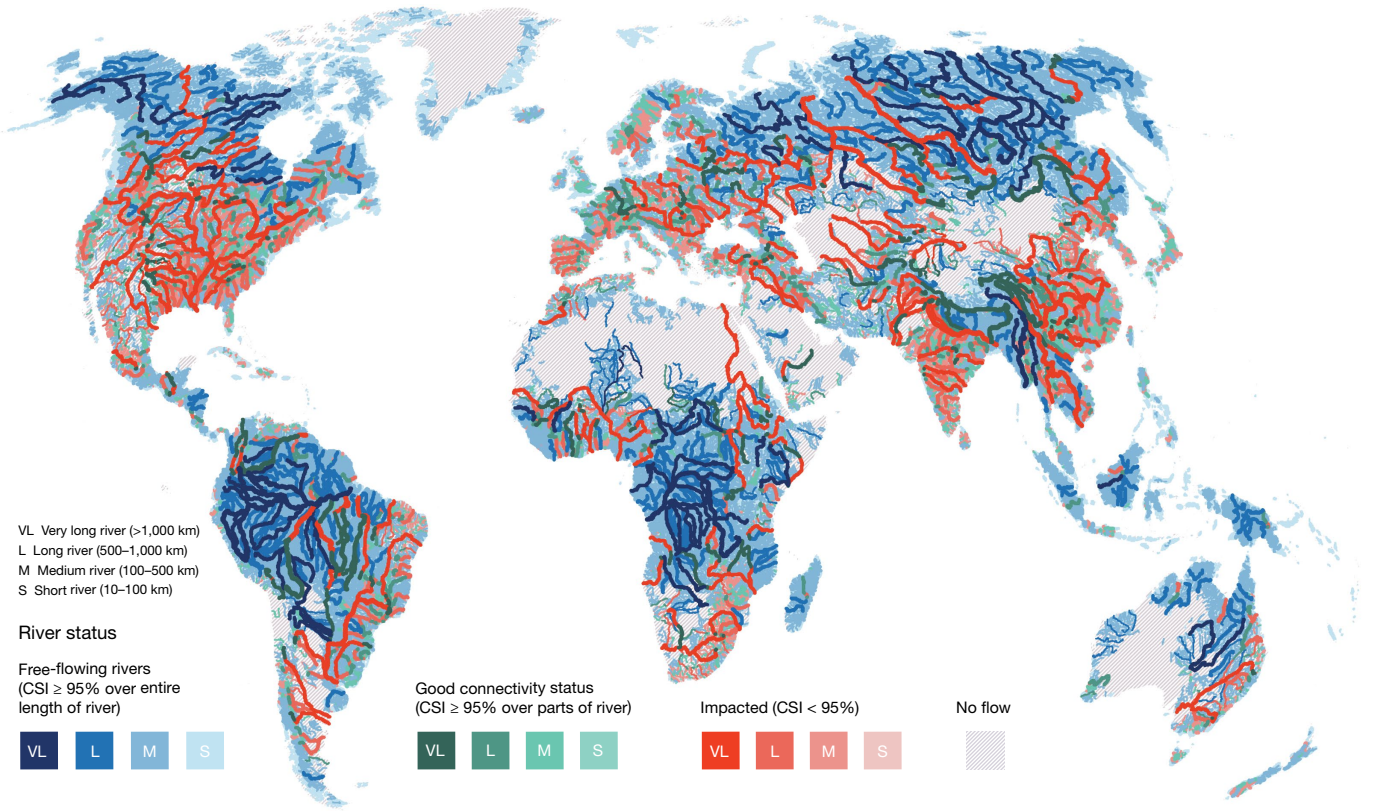


Fig. 3 | Map of the world's free-flowing rivers. This map shows the global distribution of FFRs, contiguous river stretches with good connectivity status and impacted rivers with reduced connectivity. Rivers that are not free-flowing over their entire length (that is, partially below the CSI threshold) are divided into stretches with good connectivity status (that is, the connectivity status remains above the threshold throughout the stretch; green colours) and stretches where the connectivity status is below the CSI threshold (red colours). A list of FFRs longer than 500 km is given in Supplementary Table 1.

sensitivity assessments to test the robustness of our results, and we quantified the modelled upstream effects of fragmentation, which represent a particularly novel and uncertain aspect (see Methods). Our evaluations generally indicate that the proposed indices are adequate surrogates for the selected pressure factors at the global scale. However, we advise careful interpretation of the results at smaller scales, unless additional confirmation through local validation is achieved, and we propose that national or regional studies use adjusted parameter settings informed by local knowledge.

To guide the development and test the performance of our global approach at different scales, we conducted three case studies for large (Tapajos, Brazil), medium (Luangwa, Zambia) and small (headwaters of Ganges, India) river basins, where we piloted the methodology with additional local information. Empirical application of our methods in these regions helped to improve the identification and evaluation of FFRs worldwide, in particular for short rivers. The results from these case studies indicate that our global methodology is robust for long rivers and scalable to regional and local studies if additional data are available.

The CSI and FFR methodologies presented here provide metrics for evaluating river connectivity as one of the fundamental components of ecosystem health[17,34,35]. However, a comprehensive evaluation of river health should include other components—such as water quality, land use and an assessment of biological and ecological conditions, including invasive species—that also shape ecosystem integrity[36]. Nonetheless, the river connectivity metrics provided here are considered to be key components in any future comprehensive investigation of river health, locally and globally. Furthermore, it should be noted that artificial increases in connectivity, such as those caused by inter-basin canal systems and water-transfer schemes or by constant water release from dams in naturally intermittent streams, can also compromise ecosystem health[37] or favour the spread of invasive species[38].

A global conservation challenge

With their numbers reduced to 37%, very long FFRs (>1,000 km) have become increasingly rare and remain prevalent only in remote areas of the world that are difficult to exploit economically (for example, the Arctic), in rivers too large to be developed by current technology (although this is changing as engineering techniques advance) or in less developed regions (for example, the Congo region). Of special concern is the loss of connectivity of very long and long rivers to the sea because they are of vital importance for the exchange of water, nutrients, sediments and species with deltas, estuaries and the ocean. Some remaining long FFRs deliver disproportionately high levels of certain ecosystem services, most notably inland and floodplain fisheries, sediment transport and biodiversity[18,19,24]. For example, the last two remaining very long FFRs in Southeast Asia—the Irrawaddy and Salween rivers—are critical sources of protein from inland fisheries, providing more than 1.2 million tonnes of catch annually[39], and their flow regimes maintain extensive floodplain agriculture in a region inhabited by more than 30 million people.

Given the importance of FFRs, plans to rapidly develop new infrastructure in basins around the world should be accompanied by comprehensive strategic and transboundary impact assessments and consider alternative development pathways to minimize harmful consequences[40,41]. In a world of accelerating hydropower development[42] and a shift to low-carbon economies, forward-looking system-scale approaches to energy and hydropower planning, including multi-objective trade-off analyses, are required to minimize loss of river functions while meeting energy targets[43]. Equally important is the need to find sustainable solutions to close the gap between irrigation demand and extreme water stress[44]. Our data, methods and results can play a critical part in such efforts, prioritizing rivers with high conservation value for protection and optimizing the informed selection of low-impact infrastructure developments. In a decision-making context

at national or basin scales, we recommend applying the proposed methods using finer-resolution or higher-quality data (for example, measured instead of modelled discharge), replacing proxy indicators with more explicit substitutes (for example, levees and culverts instead of urbanization and roads), using additional information on variables not available at the global scale (for example, location and storage volume of small dams, operating rules of reservoirs) and adjusting pressure-indicator settings and weightings to better reflect their local importance (for example, by considering known migratory pathways of fish).

In addition, by using more detailed local or regional data, our framework could be applied to target restoration interventions towards locations or methods that improve connectivity most effectively[45,46]. New and existing algorithms could assist in finding strategies to restore or retrofit affected river systems, such as by minimizing flow regulation, strategic removal of dams or levees (especially where they are obsolete or where maintenance is disproportionately costly) or designing and constructing more effective fish passages that would deliver the greatest return in terms of increasing CSI as well as offering some assurance of effectiveness[47,48].

The CSI is a novel metric that offers a range of opportunities for future application. It provides a comprehensive characterization of every individual river reach, unlike previous efforts that focused primarily on the assessment of longitudinal dam impacts or provided metrics only at lumped-basin scales. Although the role of dams in river fragmentation and flow regulation has been shown to be prevalent (Fig. 2), the CSI also accounts for other factors that disrupt the longitudinal, lateral, vertical and temporal components of connectivity. On the basis of the CSI, our novel and integrated method for quantifying connectivity enables the assessment of rivers across multiple scales, from individual reaches of less than one kilometre length to rivers longer than 1,000 km, with discharges spanning more than seven orders of magnitude.

Looking forward

Global environmental change, including climate and land use change, will further increase the pressure on rivers and their connectivity through alterations in flow patterns and intermittency, modifications in the frequency, magnitude and timing of droughts or floods, and changes to water quality and biological communities[30]. FFRs may increase the resilience of aquatic and riparian ecosystems under these added stresses because they provide open pathways for species movement to suitable habitats in other parts of the basin in response to rising temperatures or other changing conditions[49]. To maintain this resilience, infrastructure planning and decision making should maintain connected networks of rivers and include scenarios of future environmental change in development plans.

The international community is committed to protecting and restoring rivers under Agenda 2030 for Sustainable Development, which calls on all countries to track, at a national scale, the spatial extent and condition of water-related ecosystems[50]. The present study delivers methods and data necessary for defining the baseline and for tracking changes in the connectivity status of rivers, and comprehensively identifies the distribution and extent of globally remaining FFRs. Given the current status and future perspective, action is needed to protect or restore these threatened fluvial systems, which provide some of the most diverse and dynamic environments worldwide.

Online content

Any methods, additional references, Nature Research reporting summaries, source data, statements of data availability and associated accession codes are available at https://doi.org/10.1038/s41586-019-1111-9.

Received: 10 May 2018; Accepted: 6 March 2019;
Published online 8 May 2019.

1. Ripl, W. Water: the bloodstream of the biosphere. *Philos. Trans. R. Soc. B.* **358**, 1921–1934 (2003).
2. Lehner, B. et al. High-resolution mapping of the world's reservoirs and dams for sustainable river-flow management. *Front. Ecol. Environ.* **9**, 494–502 (2011).
3. Nilsson, C. et al. Forecasting environmental responses to restoration of rivers used as log floatways: an interdisciplinary challenge. *Ecosystems* **8**, 779–800 (2005).
4. Revenga, C., Brunner, J., Henninger, N., Kassem, K. & Payne, R. *Freshwater Systems.* Report No. 1569734607 (World Resources Institute, 2000).
5. Dudgeon, D. et al. Freshwater biodiversity: importance, threats, status and conservation challenges. *Biol. Rev. Camb. Philos. Soc.* **81**, 163–182 (2006).
6. Cardinale, B. J. et al. Biodiversity loss and its impact on humanity. *Nature* **486**, 59–67 (2012); corrigendum **489**, 326 (2012).
7. Ward, J. V. & Stanford, J. A. The serial discontinuity concept: extending the model to floodplain rivers. *Regul. Rivers Res. Manage.* **10**, 159–168 (1995).
8. Ward, J. V. The four-dimensional nature of lotic ecosystems. *J. N. Am. Benthol. Soc.* **8**, 2 (1989).
9. Poff, N. L. et al. The natural flow regime: a paradigm for river conservation and restoration. *Bioscience* **47**, 769–784 (1997).
10. Pringle, C. M. What is hydrologic connectivity and why is it ecologically important? *Hydrol. Processes* **17**, 2685–2689 (2003).
11. Nilsson, C. & Berggren, K. Alterations of riparian ecosystems caused by river regulation. *Bioscience* **50**, 783–792 (2000).
12. Olden, J. D. in *Conservation of Freshwater Fishes: Challenges and Opportunities for Fish Conservation in Dam-impacted Waters* (eds Closs, G. P. et al.) 107–148 (Cambridge Univ. Press, Cambridge, 2016).
13. Costanza, R. et al. The value of the world's ecosystem services and natural capital. *Nature* **387**, 253–260 (1997).
14. Opperman, J. J., Moyle, P. B., Larsen, E. W., Florsheim, J. L. & Manfree, A. D. *Floodplains: Processes and Management for Ecosystem Services* (Univ. California Press, Oakland, 2017).
15. Benchimol, M. & Peres, C. A. Widespread forest vertebrate extinctions induced by a mega hydroelectric dam in lowland Amazonia. *PLoS One* **10**, e0129818 (2015).
16. Lees, A. C., Peres, C. A., Fearnside, P. M., Schneider, M. & Zuanon, J. A. S. Hydropower and the future of Amazonian biodiversity. *Biodivers. Conserv.* **25**, 451–466 (2016).
17. Vörösmarty, C. J. et al. Global threats to human water security and river biodiversity. *Nature* **467**, 555–561 (2010).
18. Syvitski, J. P. M. et al. Sinking deltas due to human activities. *Nat. Geosci.* **2**, 681–686 (2009).
19. McIntyre, P. B., Reidy Liermann, C. A. & Revenga, C. Linking freshwater fishery management to global food security and biodiversity conservation. *Proc. Natl Acad. Sci. USA* **113**, 12880–12885 (2016).
20. Auerbach, D. A., Deisenroth, D. B., McShane, R. R., McCluney, K. E. & Poff, N. L. Beyond the concrete: accounting for ecosystem services from free-flowing rivers. *Ecosyst. Serv.* **10**, 1–5 (2014).
21. Arthington, A. H. et al. The Brisbane declaration and global action agenda on environmental flows (2018). *Front. Environ. Sci.* **6** 45 (2018).
22. Zarfl, C., Lumsdon, A. E., Berlekamp, J., Tydecks, L. & Tockner, K. A global boom in hydropower dam construction. *Aquat. Sci.* **77**, 161–170 (2015).
23. Adams, K. et al. *2017 Hydropower Status Report* (International Hydropower Association, 2017); https://www.hydropower.org/sites/default/files/publications-docs/2017HydropowerStatusReport.pdf.
24. Winemiller, K. O. et al. Balancing hydropower and biodiversity in the Amazon, Congo, and Mekong. *Science* **351**, 128–129 (2016).
25. Shumilova, O., Tockner, K., Thieme, M., Koska, A. & Zarfl, C. Global water transfer megaprojects: a potential solution for the water-food-energy nexus? *Front. Environ. Sci.* **6**, 150 (2018).
26. Grill, G. et al. An index-based framework for assessing patterns and trends in river fragmentation and flow regulation by global dams at multiple scales. *Environ. Res. Lett.* **10**, 015001 (2015).
27. Nilsson, C., Reidy, C. A., Dynesius, M. & Revenga, C. Fragmentation and flow regulation of the world's large river systems. *Science* **308**, 405–408 (2005).
28. Reidy Liermann, C., Nilsson, C., Robertson, J. & Ng, R. Y. Implications of dam obstruction for global freshwater fish diversity. *Bioscience* **62**, 539–548 (2012).
29. Lehner, B. & Grill, G. Global river hydrography and network routing: baseline data and new approaches to study the world's large river systems. *Hydrol. Processes* **27**, 2171–2186 (2013).
30. Palmer, M. A. et al. Climate change and the world's river basins: anticipating management options. *Front. Ecol. Environ.* **6**, 81–89 (2008).
31. Lehner, B., Verdin, K. & Jarvis, A. New global hydrography derived from spaceborne elevation data. *Eos* **89**, 93 (2008).
32. Mulligan, M., Saenz-Cruz, L., van Soesbergen, A., Smith, V. T. & Zurita, L. Global dam database and Geowiki, version 1 http://globaldamwatch.org/ (2009).
33. Couto, T. B. A. & Olden, J. D. Global proliferation of small hydropower plants: science and policy. *Front. Ecol. Environ.* **16**, 91–100 (2018).
34. Karr, J. Biological integrity: a long neglected aspect of water resource management. *Ecol. Appl.* **1**, 66–84 (1991).
35. Poff, N. L. Landscape filters and species traits: towards mechanistic understanding and prediction in stream ecology. *J. N. Am. Benthol. Soc.* **16**, 391–409 (1997).
36. Kuehne, L. M., Olden, J. D., Strecker, A. L., Lawler, J. J. & Theobald, D. M. Past, present, and future of ecological integrity assessment for fresh waters. *Front. Ecol. Environ.* **15**, 197–205 (2017).
37. Zhuang, W. Eco-environmental impact of inter-basin water transfer projects: a review. *Environ. Sci. Pollut. Res. Int.* **23**, 12867–12879 (2016).

38. Gallardo, B. & Aldridge, D. C. Inter-basin water transfers and the expansion of aquatic invasive species. *Water Res.* **143**, 282–291 (2018).
39. Bartley, D. M., De Graaf, G. J., Valbo-Jorgensen, J. & Marmulla, G. Inland capture fisheries: status and data issues. *Fish. Manag. Ecol.* **22**, 71–77 (2015).
40. Ziv, G., Baran, E., Nam, S., Rodríguez-Iturbe, I. & Levin, S. A. Trading-off fish biodiversity, food security, and hydropower in the Mekong River Basin. *Proc. Natl Acad. Sci. USA* **109**, 5609–5614 (2012).
41. Schmitt, R. J., Bizzi, S., Castelletti, A. & Kondolf, G. Improved trade-offs of hydropower and sand connectivity by strategic dam planning in the Mekong. *Nat. Sustainability* **1**, 96–104 (2018).
42. US Energy Information Administration. *International Energy Outlook.* Report No. DOE/EIA-0484 (US Energy Information Administration, 2016).
43. Opperman, J., Grill, G. & Hartmann, J. *The Power of Rivers: Finding Balance Between Energy and Conservation in Hydropower Development* (The Nature Conservancy, Washington, DC, 2015).
44. Jägermeyr, J., Pastor, A., Biemans, H. & Gerten, D. Reconciling irrigated food production with environmental flows for Sustainable Development Goals implementation. *Nat. Commun.* **8**, 15900 (2017).
45. Palmer, M. A., Hondula, K. L. & Koch, B. J. Ecological restoration of streams and rivers: shifting strategies and shifting goals. *Annu. Rev. Ecol. Evol. Syst.* **45**, 247–269 (2014).
46. Magilligan, F. J. et al. River restoration by dam removal: enhancing connectivity at watershed scales. *Elem. Sci. Anth.* **4**, 000108 (2016).
47. Kemp, P. S. & O'Hanley, J. R. Procedures for evaluating and prioritising the removal of fish passage barriers: a synthesis. *Fish. Manag. Ecol.* **17**, 297–322 (2010).
48. Sheer, M. B. & Steel, E. A. Lost watersheds: barriers, aquatic habitat connectivity, and salmon persistence in the Willamette and Lower Columbia River basins. *Trans. Am. Fisheries Soc.* **135**, 1654–1669 (2006).
49. Groves, C. R. et al. Incorporating climate change into systematic conservation planning. *Biodivers. Conserv.* **21**, 1651–1671 (2012).
50. UN Water Integrated Monitoring Guide for SDG 6 (UN Water, 2017); http://www.unwater.org/publications/integrated-monitoring-guide-sdg-6.

Acknowledgements Funding for this study was provided in part by World Wildlife Fund (WWF), the Natural Sciences and Engineering Research Council of Canada (NSERC Discovery Grant RGPIN/341992-2013) and McGill University, Montreal, Québec, Canada.

Reviewer information *Nature* thanks Edward Park, N. LeRoy Poff and the other anonymous reviewer(s) for their contribution to the peer review of this work.

Author contributions G.G., B. Lehner, M.T., B.G. and D.T. led and designed the study. G.G. and B. Lehner performed the analysis. G.G., B. Lehner, M.T., C.N., K.T. and C.Z. wrote the initial draft of the manuscript with input from all other authors. M.T., B.G., D.T., C.R.L., J.S. and K.T. revised and edited the manuscript. Z.H., J.M., C.N., J.D.O., P.P. and L.S. advised on fragmentation indicator design and implementation. P.B., H.E.M., M.G., R.J.P.S. and F.T. advised on sediment indicator design and implementation. M.T., B.G., J.H., M.E.M., J.J.O. and P.S. wrote policy recommendations and conclusions. F.A., S.B., H.C., R.F., S.S.-R. and P.H.V. contributed to case study design, implementation and validation. P.B., L.C., B. Lip, M.M., A.v.S. and C.Z. contributed essential data layers for the analysis.

Competing interests The authors declare no competing interests.

Additional information
Extended data is available for this paper at https://doi.org/10.1038/s41586-019-1111-9.
Supplementary information is available for this paper at https://doi.org/10.1038/s41586-019-1111-9.
Reprints and permissions information is available at http://www.nature.com/reprints.
Correspondence and requests for materials should be addressed to G.G. or B. Lehner.
Publisher's note: Springer Nature remains neutral with regard to jurisdictional claims in published maps and institutional affiliations.

© The Author(s), under exclusive licence to Springer Nature Limited 2019

METHODS

Overview. The methodology of our assessment was collaboratively developed over the course of three years by a group of over 30 scientists, conservation practitioners and industry representatives, in an attempt to update an earlier global assessment of FFRs[51]. The main steps are detailed below and depicted in Extended Data Fig. 1. We first developed a comprehensive definition of FFRs (step 1) including multiple aspects of connectivity. Next, we identified five major pressure factors (step 2) that influence river connectivity according to an extensive literature review. These pressure factors are: (1) river fragmentation, (2) flow regulation, (3) sediment trapping, (4) water consumption (surface or groundwater abstractions) and (5) infrastructure development in riparian and floodplain areas. We selected these factors to cover the full spectrum of impacts on river connectivity while attempting to avoid inter-correlation among factors—although we acknowledge that some level of inter-correlation is inherent owing to the general global drivers of human population densities and economic development.

To quantify each pressure factor, we calculated six proxy indicators (step 3) using data from available global remote-sensing products, other data compilations, or numerical model outputs, such as discharge simulations (Extended Data Table 1). The pressure factor for infrastructure development in riparian and floodplain areas has two pressure indicators to more broadly cover the different types of infrastructure development in these areas. We specifically chose indicators that we expect to have substantial influence on connectivity and can be generated using robust global datasets of sufficient quality and consistency between countries and regions. All pressure indicators were calculated for every river reach of the global river network.

Guided by literature reviews and expert judgement, we then developed a weighting model to combine the six pressure indicators (step 4). We developed 100 weighting scenarios and tested different thresholds to yield a best match between the resulting FFRs and a benchmarking dataset of reported FFRs compiled from literature resources and expert input.

The final selection of weights was applied in a multi-criteria average calculation to derive the CSI for every river reach (step 5). The CSI ranges from 0% to 100%, the latter indicating full connectivity. Only river reaches with a CSI of ≥95% were considered as having good connectivity status whereas river reaches below 95% were classified as impacted (step 6). Finally, river reaches were aggregated into rivers, that is, contiguous flow paths from the source to the river outlet. If a river is at or above the CSI threshold of 95% over its entire length it is declared to be an FFR. Otherwise, the river is declared not free-flowing, yet it can maintain a mix of stretches with good connectivity status and stretches that are impacted.

Hydrographic framework. We integrated all indicator datasets in our modelling framework using the spatial units of the HydroSHEDS database. HydroSHEDS is a hydrographic mapping product that provides river and catchment information for regional and global-scale applications in a consistent format[31], including catchment areas and discharge estimates. For this study, we extracted a global river network from the provided drainage direction grid at 500 m pixel resolution by defining streams as all pixels that exceed a long-term average natural discharge of 0.1 $m^3 s^{-1}$ or an upstream catchment area of 10 km^2. We refrained from including streams below these thresholds as they are increasingly unreliable in their representation through global datasets. These selection criteria resulted in 8,477,883 individual river reaches (that is, line segments between confluences) with an average length of 4.2 km (s.d. = 4.8 km), totalling 35.9 million kilometres of river network. Each river reach is linked to a polygon of its contributing hydrological sub-catchment, with an average area of about 12 km^2.

For the purpose of this paper, we define a 'river reach' as a cartographic—rather than a functional—unit, represented by the smallest spatial element of our global river network, that is, the line segment between two neighbouring confluences; a 'river stretch' as two or more contiguous reaches, but not a full river; and a 'river' as an aggregation of river reaches that form a single-threaded, contiguous flow path from the headwater source to the river outlet. The river outlet can represent the river mouth at the ocean, a terminal inland depression or the confluence with a larger river (Extended Data Fig. 2). It should be noted that although we used the full river network to conduct the initial calculations, we removed all rivers from the statistical analyses and reported results that were shorter than 10 km, showed an average annual river flow of less than 1 $m^3 s^{-1}$ or were in hot or cold deserts according to existing physiographic maps, to exclude increasingly uncertain results of smaller rivers. These selection criteria resulted in 308,015 distinct rivers with a total length of 11.7 million kilometres globally.

For every river reach, estimates of long-term (1971–2000) discharge averages have been derived through a geospatial downscaling procedure[29] from the 0.5°-resolution runoff and discharge layers of the global WaterGAP model (version 2.2 of 2014)[52]. WaterGAP is a well documented and validated integrated water-balance model that simulates both natural discharge (that is, without human modifications) and anthropogenic discharge; for the latter, consumptive water use—that is, total water abstractions minus return flows—are calculated for agricultural (mostly irrigation), industrial and municipal sectors[53]. A validation of the downscaled discharge estimates against observations at 3,003 global gauging stations[54], representing river sizes from 0.004 to 180,000 $m^3 s^{-1}$, confirmed good overall correlations for long-term average discharges ($R^2 = 0.99$ with 0.2% positive bias and a symmetric mean absolute percentage error sMAPE[55] of 35%, improving to 13% for rivers ≥100 $m^3 s^{-1}$).

For all network calculations, we applied the global river routing model HydroROUT[26], which is built upon the HydroSHEDS database and features a nested, multi-scale model approach and advanced implementation of connectivity and uses a novel object-oriented vector data structure in a graph–theoretical framework. HydroROUT was implemented in this study to calculate indicators at the river reach scale as described below.

Pressure indicators. *Degree of fragmentation (DOF).* River fragmentation indices typically measure the degree to which river networks are fragmented longitudinally by infrastructure, such as hydropower and irrigation dams. Fragmentation prevents effective ecological processes that depend on longitudinal river connectivity, including transport of organic and inorganic matter and upstream and downstream movements of aquatic and riparian species. Although passive movement (drifting) may be impeded primarily in the downstream direction, active movement (for example, fish migration) operates in both the up- and downstream directions, and considerable evidence points to the upstream effects of dams, such as reported changes in fish assemblage structure associated with stream bank destabilization[56], increased richness of fish macrohabitat generalists[57], decreased juvenile fish survival[58] and decreased native fish diversity[59] in streams above reservoirs.

For this study, we developed the DOF as a new index at the river-reach scale intended to characterize the magnitude and spatial extent of reduced longitudinal connectivity due to anthropogenic barriers in the river channel. It identifies river reaches up- and downstream of a dam or impoundment as being fragmented, and it assigns levels of fragmentation based on the 'distance' from the impact location, which we determine by measuring the dissimilarity of river sizes in terms of flow quantities.

We suggest that: (1) river discharge can serve as a coarse proxy for the occurrence of species assemblages that utilize a certain range of river flow[60]; (2) discharge can also serve as a proxy for 'distance' in the traditional (spatial) sense (that is, greater differences in discharge are expected at larger distances from a given location), and increasing distance allows amelioration effects of the fragmentation impact (for example, through continued water and sediment influx from new tributaries and local contributing areas); and (3) differences in discharge can serve as a proxy for environmental disparity and natural discontinuities because river stretches with highly dissimilar discharges, such as the confluence of a small tributary into a major river, are assumed to be less representative of continuous environmental conditions. We thus based the conceptual approach of calculating the DOF on the similarity of river sizes determined by their discharges. The DOF assumes that the fragmentation effect diminishes as river sizes become increasingly dissimilar from the river size at the barrier location in both the up- and downstream directions (Extended Data Fig. 3).

Guided by the involved expert group and the explicit examination of case studies from the Tapajos, Luangwa and Ganges rivers, we tested several options (Extended Data Fig. 3c) and finally applied a fivefold (that is, half order of magnitude) increase or decrease in discharge as the maximum discharge range (dr) in which impacts of the DOF would appear (that is, dr = 5 in equation (1) below). A logarithmic, rather than linear, decay function was chosen to calculate the DOF values to better appropriate typical growth and decline rates of dendritic network structures. The DOF was scaled to values between 0% and 100% and was calculated for an individual barrier in both the up- and downstream directions as:

$$\mathrm{DOF}_j = 100 - \frac{|\log_{10} d_{\mathrm{bloc}} - \log_{10} d_j| \times 100}{\log_{10}(\mathrm{dr})} \quad (1)$$

where DOF_j is the DOF at river reach j up- or downstream of the barrier, d_j is the natural average discharge of river reach j, d_{bloc} is the natural average discharge at the location of the barrier under investigation and dr is the maximum discharge range beyond which no fragmentation effects are expected. In reaches where DOF values of multiple barriers overlap, the maximum value is applied.

For the DOF analysis we included 6,849 large dams (≥15 m high and ≥0.1 km^3 storage capacity, with few exceptions) as compiled in the Global Reservoir and Dam (GRanD) database[2] after removing a small number of dams with undefined status. We also added 13,195 dams from the GlObal geOreferenced Database of Dams (GOODD)[32] representing medium-size dams that are visible on global remote-sensing imagery and that we confirmed against existing reservoir polygons of the HydroLAKES database[61]. An additional 76 dams were added to account for the construction of large dams in key rivers since the publication of the databases.

Also, for the first time in a global study, the natural fragmentation effect of waterfalls was taken into account by incorporating a global database of 4,055 waterfalls[62]. After removing records that were flagged as uncertain, 2,436 waterfalls were

geo-located to our river reaches. The underlying premise is that waterfalls act as natural discontinuities, hence the fragmentation effect of artificial dams should not extend beyond the existing barrier; for example, a dam just downstream of a waterfall should not be considered to affect the river upstream of the fall. Because the barrier effect from waterfalls accounts primarily in the upstream direction, the DOF algorithm was modified to stop extending upstream if encountering the location of a waterfall, whereas no waterfall effect was assumed in the downstream direction.

Degree of regulation (DOR). The DOR provides an index to quantify how the storage of water in a dam or set of dams can alter the natural flow regime of downstream river reaches[2,63]. While fragmentation (DOF) measures the longitudinal effects caused by barriers, flow regulation (DOR) affects primarily lateral and temporal connectivity as, for example, the reduction of peak flows impedes species movement and exchange of materials and energy to and from floodplains. Furthermore, temporal connectivity can be altered due to delayed release patterns and resulting shifts in the timing of flow events.

The concept of the index is based on the relationship between the storage volume of a reservoir and the total annual river flow volume at the dam's location, and is expressed as the percentage of river flow volume that can be withheld in the dam's reservoir, represented by:

$$\mathrm{DOR}_j = 100 \times \frac{\sum_{i=1}^{n} \mathrm{svol}_i}{d_{\mathrm{vol}}} \tag{2}$$

where DOR_j is the DOR at river reach j, svol_i is the storage volume of any reservoir i upstream of river reach j, n is the total number of reservoirs upstream of river reach j, and d_{vol} is the natural average discharge volume per year at river reach j. The underlying assumption is that a large reservoir on a river with low annual discharge will generally have a larger regulatory effect on the natural flow regime than a small reservoir on a river with higher flow rates.

In this study, we capped the DOR at 100%, which limits all multi-year reservoirs to the same maximum DOR. We used the same selection of 20,120 dams for DOR calculations as described for the DOF above. Reservoir storage capacities were either taken directly from the available GRanD records or, in the case of GOODD, estimated from reservoir areas (as provided by HydroLAKES) using statistical approaches[2].

Sediment trapping index (SED). Sediment connectivity is a key driver for morphodynamic processes in small upland streams, as well as in large lowland rivers[64,65], which eventually form the physical template for fluvial ecosystems. Dams have been shown to capture large amounts of sediments in their reservoir impoundment[66], with the amount of sediment being trapped determined by dam design and operation and by the spatial heterogeneity of natural sediment flux in the river network[41]. This sediment capture can trigger a cascade of impacts on fluvio-geomorphological dynamics and processes far downstream, and reduce sediment delivery for floodplains and deltas alike[67], ultimately impacting coastal morphology and leading to increased rates of delta subsidence and coastal erosion[18,68,69].

Owing to data limitations, the deterministic modelling of sediment transport processes in individual river reaches is currently limited to regional scales[70,71]. Here we developed a novel global index, SED, as a proxy of dam impacts on longitudinal sediment fluxes in a river network. The SED quantifies the proportion of potential sediment load (PSL) trapped by dams at any given point in the river system (see Extended Data Fig. 4). It focuses on suspended load because there are currently not enough observations to build a model for the partitioning between bed-load and suspended load on global scales[72]. The SED therefore provides a lower-bound estimate for dam impacts on river sediment budgets, not considering the trapping of around 1%–5% of the total sediment load (for large rivers) transported as bed-load[72].

Because the PSL in rivers is driven by sediment supply, we used a high-resolution (250 m) global erosion map as a proxy to calculate the sediment supply to rivers. The erosion map combines natural forcing factors—such as erosivity, topographical conditions of the hill slopes and soil properties with land use, cropping systems and conservation practices[73]—and considers mobilization of sediment from sheet and rill erosion, but neglects denudation and fluvial conveyance processes. Despite these limitations, the spatially explicit estimates of sediment displacement represent an indicator to quantify the potential spatial variability in sediment supply within basins.

We used the erosion map in our global routing model to quantify the accumulated sediment load in the river system at each river reach, and we accounted for both natural and artificial sediment trapping in lakes and reservoirs by multiplying the accumulated sediment loads with respective trapping efficiencies. The PSL values were calculated in a recursive process from upstream to downstream reaches as:

$$\mathrm{PSL}_j = \left(\sum_{i=1}^{n} \mathrm{PSL}_i + \mathrm{ss}_j\right) \times (1 - \mathrm{TE}_{\mathrm{lak},j}) \tag{3}$$

where PSL_j is the PSL of reach j, PSL_i is the PSL of each directly contributing upstream reach i after lake trapping, n is the number of directly contributing upstream reaches, ss_j is the sediment supply from local erosion in the sub-catchment of reach j and $\mathrm{TE}_{\mathrm{lak},j}$ is the trapping efficiency of all lakes located on reach j.

We then calculated the modified sediment load (MSL), which represents the sediment load after trapping in reservoirs, again using a recursive upstream-to-downstream approach, as:

$$\mathrm{MSL}_j = \left[\left(\sum_{i=1}^{n} \mathrm{MSL}_i\right) + \mathrm{ss}_j\right] \times (1 - \mathrm{TE}_{\mathrm{lak+res},j}) \tag{4}$$

where MSL_j is the MSL of reach j, MSL_i is the MSL of each directly contributing upstream reach i after lake and reservoir trapping, n is the number of directly contributing upstream reaches, ss_j is the sediment supply from accumulated erosion of reach j and $\mathrm{TE}_{\mathrm{lak+res},j}$ is the trapping efficiency of all lakes and reservoirs combined on reach j.

Trapping efficiencies for lakes and reservoirs were calculated following the method proposed by Brune[74], using storage volumes provided by GRanD and HydroLAKES and described for the DOR above. Brune's method is widely applied and has been found to provide reasonable estimates of long-term mean trapping efficiencies[66,75,76]. It is expressed as:

$$\mathrm{TE}_j = 1 - \frac{0.05}{\sqrt{\Delta\tau_j}} \tag{5}$$

with

$$\Delta\tau_j = \frac{\mathrm{svol}_j}{d_j} \tag{6}$$

where TE_j is the trapping efficiency of lakes and/or reservoirs located on reach j, $\Delta\tau_j$ is the local residence time change at river reach j in years, svol_j is the total storage capacity of all lakes and/or reservoirs on reach j and d_j is the discharge at the mouth of reach j.

Finally, we calculated the SED as a percentage value between 0% and 100% for every river reach:

$$\mathrm{SED}_j = \frac{\mathrm{PSL}_j - \mathrm{MSL}_j}{\mathrm{PSL}_j} \times 100 \tag{7}$$

To test the quality of our global sediment model results, we compared the PSL estimates against reported data of observed sediment transport at 398 gauging stations globally[64,77–79]. Our estimates were able to explain 64% of global and 65% of continental variance in observed sediment load and more than 83% for three continents (North America, Asia and Europe). However, the intra-basin variance is most relevant to derive a plausible indicator for natural sediment origins and spatial patterns of sediment connectivity within individual river basins. Within three river basins with multiple observations (Blue Nile and Niger in Africa and Amazon in South America) and for four Asian river basins (Mekong, Irrawaddy, Salween and Red River), the modelled PSL explains on average 81% of the observed intra-basin variance, indicating a reasonable performance of our global sediment model.

To test the results of the modelled sediment trapping, we compared our results against 34 reported values for major global rivers (including Yangtze, Madeira, Mekong) as found in the literature[70,74,80–85]. Our index was able to explain 76% of the variance indicating that the SED is a suitable proxy for dam impacts on sediment fluxes in global river networks.

Consumptive water use (USE). Water consumption for irrigation, industry, municipal uses and water transfer to other river systems may affect lateral connectivity as reduced flows limit access to riparian areas, and has implications on vertical connectivity through changes in groundwater recharge and evaporation. The timing and seasonality of water abstractions (for example, for irrigation purposes) can also alter temporal connectivity, and in cases where all water is consumed and rivers fall dry, even longitudinal connectivity is impeded, as evidenced by rivers such as the Colorado failing to reach the ocean owing to over-use.

Using downscaled outputs from the WaterGAP model (for details, see section 'Hydrographic framework'), we calculated water consumptive loss for our high-resolution river network. The results provide for every river reach the long-term average reduction of river discharge due to anthropogenic water consumption as a percentage of natural flow:

$$\mathrm{USE}_j = 100 \times \frac{d_{\mathrm{nat}} - d_{\mathrm{ant}}}{d_{\mathrm{nat}}} \tag{8}$$

where USE_j is the consumptive water use at river reach j, d_{nat} represents the natural long-term discharge without human influences and d_{ant} represents the average long-term discharge after human abstractions and use.

Road density (RDD). Road density is a proxy for lateral disconnection from floodplains and longitudinal loss of connectivity at intersections with streams, in particular culverts. We used the vector dataset produced by the Global Road Inventory Project (GRIP, version 3)[86]. The classified road categories 'freeways', 'primary', 'secondary' and 'tertiary' were treated as equally important in our density calculations, whereas the category 'local, residential and urban roads' was excluded to avoid collinearity effects with the urban areas (see below). We summarized the road density within a 1-km buffer around each river reach to produce an estimate of average road density (in percentage of surface area covered, assuming an average road width of 50 m) per river reach.

To eliminate isolated outlier effects on short river reaches (which in some instances can show disproportionally high road density values owing to geometric artefacts, rather than to real situations), we applied a customized geospatial filter for all river reaches <3 km in length: we compared every river reach value with its direct upstream and downstream neighbouring river reach; if the centre river reach showed a value that differed greatly (>15%) from the (length-weighted) average of the two neighbouring values, the centre value was replaced with that average. We applied these adjustments to the road density and nightlight intensity layers (see below), resulting in corrections of 0.0003% and 0.006% of affected river reaches, respectively.

Urban areas (URB). Urban areas and cities can affect lateral connectivity by reducing floodplain access owing to paving and urban infrastructure, as well as through artificial channelization or levee construction that confines the river bed and/or affects river meandering[87]. Several studies on urbanization and rivers show that about 10% of contiguous impervious area within a catchment typically causes an observable and probably irreversible river degradation and loss of ecosystem functions[88–90]. It should be noted that the URB is considered to be only a weak indicator for levee construction, yet no explicit and comprehensive data on levees or dykes exist globally.

As a proxy for urban effects on lateral river connectivity, we opted to use the global dataset of nightlight intensity data (DMSP-OLS version 4)[91], which blends information on the degree of urbanization and the level of economic development[92]. We accounted for the 'light-bleeding' effect into adjacent areas[93] by clipping the nightlights dataset using a MODIS-based urban extent layer[94]. We summarized the data within the contributing sub-catchment of each river reach to produce an average nightlight intensity for each river reach and applied the outlier correction as described in section 'Road density (RDD)'.

Determination of CSI. *Index calculation.* The conceptual approach to calculate a combined CSI for every river reach is to produce a weighted average of the six individual pressure indicators, each defined within a range of 0%–100%, and to subtract it from the maximum of 100%:

$$\mathrm{CSI}_j = 100 - \frac{\sum_{i=1}^{n} x_{i,j} w_i}{\sum_{i=1}^{n} w_i} \quad (9)$$

where CSI_j is the CSI at river reach j, $x_{i,j}$ is the value of pressure indicator i at reach j, w_i is the weight applied to the pressure indicator i and n is the number of pressure indicators (in our case, 6). We prescribe the sum of w_i to be 100%, hence the resulting CSI values can range from 0% (not connected) to 100% (fully connected). For each pressure indicator, values below 0.1% were set to 0% so that rivers with only minimal impacts remain fully connected. For example, small DOR values below 0.1% occur in large downstream rivers affected by small and far-away headwater dams.

For the pressure indicators RDD and URB, we applied a modification that allows amplification of the indicator by a factor that is proportional to the extent of floodplains around the river, assuming that roads and urban development within floodplains are particularly likely to affect latitudinal connectivity. We used the long-term maximum inundation extent provided in the global inundation map GIEMS-D15[95] and allowed a maximum increase of the indicator by a factor of 1.5 (with a cap at 100%) if all roads or urban areas are inside floodplains:

$$x_{i,j} = \tilde{x}_{i,j} \times \left(1 + \frac{f_j}{2}\right) \quad (10)$$

where $x_{i,j}$ is the value of pressure indicator i (RDD or URB) at river reach j after floodplain amplification, $\tilde{x}_{i,j}$ is the value of pressure indicator i (RDD or URB) at river reach j without floodplain amplification, and f_j is the fraction of floodplain extent within the contributing sub-catchment of river reach j.

The approach of calculating CSI as a weighted average poses the challenge of finding appropriate weights for each pressure indicator. To achieve this, we first created a representative sample of 100 random and unique scenarios where the six weights oscillated freely in 5% intervals (minimum, 5%; maximum, 75%). For the final weight selection, we considered all scenarios that best reproduced the FFR status of a set of benchmark rivers that were reported to be free-flowing (for more details, see section 'Benchmarking and weighting'), and among those we chose the one with the most reasonable weightings on the basis of a literature review and expert judgement.

Benchmarking and weighting. The purpose of benchmarking was to identify pressure indicator weights that, in combination with a given CSI threshold, best match the FFR status of rivers which are well known for their unaffected connectivity (as determined by expert opinion or existing assessments). For this purpose we created a reference database of benchmark FFRs using sources from Nilsson et al.[27] and from expert knowledge. The reported 160 rivers were distributed across the world and ranged from 20 km to 3,300 km in length (for a complete list see Supplementary Table 2).

To compare different weight settings, as well as to test the sensitivity of the results to those settings, we explored 100 different weighting scenarios (see Supplementary Table 3). We assigned varying weights to the individual pressure indicators and produced statistics and maps for visual inspection. To determine the level of agreement between scenario results and benchmarking rivers, we calculated the percentage of rivers which were correctly classified as free-flowing. It should be noted that all 100 scenarios applied a CSI threshold of 95% below which a river reach is declared non-free-flowing. This threshold was determined through additional scenario assessments (not shown here) and its validity was tested in a subsequent sensitivity analysis (see section 'Sensitivity analysis').

In general, the benchmarking analysis showed high levels of agreement between the modelled and reported free-flowing status of rivers. The range of scenarios matched between 78.1% and 97.5% of benchmark FFRs, and several scenarios produced agreements of close to 97% or higher (≥155 out of 160 rivers matching; see Extended Data Table 3), which we considered equally good given the inherent model uncertainties. To choose the most plausible scenario among them, we took into account known responses of river systems according to literature. For this, we used documented evidence to identify a plausible range of limits for each individual pressure indicator beyond which that indicator alone should cause a river reach to be declared impacted; we termed this limit the 'single pressure limit' (SPL). For example, a sediment trapping of 30% or more has been linked to negative effects on aquatic ecosystems due to fluvio-geomorphological changes (Extended Data Table 4a) and can thus serve as a reasonable SPL value. An SED weight of 15%, combined with a CSI threshold of 95%, will trigger all river reaches with an SED indicator of 33.3% or higher (that is, values well aligned with the SPL range) to be non-free-flowing even if no other pressure exists; hence this weight setting is considered plausible. Guided by this approach, we chose scenario 11 as the most plausible on the basis of the following observations:

Scenario 11 results in a total of approximately 269,000 river reaches being impacted, that is, falling below the free-flowing threshold (CSI < 95%). The weight settings of this scenario are 30%, 30%, 15%, 15%, 5% and 5% for the DOF, DOR, SED, USE, RDD and URB indicators, respectively, leading to the corresponding SPL values shown in Extended Data Table 4b and discussed below.

Given the novelty of the DOF approach and the lack of comparable studies that measure fragmentation in a similar way, we cannot corroborate the associated SPL of 16.7% as being within existing literature ranges. Nonetheless, the scenario is well placed within an expert-estimated SPL range of 10%–50% (Extended Data Table 4a), and the relatively high weight is in line with the postulated wide-ranging longitudinal fragmentation effects of dams. As a result, approximately 242,000 river reaches were declared impacted owing to the DOF alone, representing 90% of all impacted river reaches (Extended Data Fig. 5a).

As for the DOR, scenario 11 assigns the same weight as for the DOF (30%). Other studies have determined effects from river regulation as low as 2%–15% (Extended Data Table 4a), fitting well with our SPL value of 16.7%. As a result, over 131,000 river reaches (49% of impacted river reaches) are impacted because of the DOR alone, making flow regulation the second most common pressure factor (Extended Data Fig. 5b).

Our literature review showed that rivers with sediment trapping as low as 30% are associated with severe losses of essential river functions, such as reduced floodplain storage and accelerated delta subsidence, ultimately leading to delta flooding and shoreline retreat (Extended Data Table 4a). Hence the weighting of the SED (15%) and the associated SPL value (33.3%) are considered plausible. A total of approximately 101,000 river reaches (38% of impacted river reaches) are impacted by the SED alone (Extended Data Fig. 5c).

For the USE, the same weight is applied as for the SED (15%) and the associated SPL value (33.3%) falls within the cited range of 10%–50% for consumptive water use as a general indicator of water stress or compromised environmental water requirements (Extended Data Table 4a). However, given that water consumption is an important factor only in relatively dry areas of the world, and that only about 20% of the river reaches affected by water consumption showed a value larger than

10%, the overall importance of this factor is relatively low, with roughly 18,000 river reaches (7% of impacted river reaches) being impacted owing to the USE alone (Extended Data Fig. 5d).

Scenario 11 assigns a low weight (5%) and accordingly high SPL threshold (100%) for the RDD, meaning that only high road densities within floodplains can cause a reach to be designated as impacted by the RDD alone. Literature sources indicate that a lower SPL value of 5%–30% may be applicable (Extended Data Table 4a), yet the lower weight of scenario 11 reflects in part the decreasing level of confidence in this proxy and the increasingly indirect effects of roads on the free-flowing status of rivers. As a result, even though roads are widespread and penetrate even remote areas, we did not identify river reaches where the RDD alone was causing a river reach to become not free-flowing. Nevertheless, the RDD does contribute to lowering the CSI values of affected river reaches (Extended Data Fig. 5e).

Because the confidence in the proxy of nightlight intensity in urban areas is similarly low as for RDD, the low weight (5%) and high SPL threshold (100%) assigned by scenario 11 to the URB are considered in line with general ranges found in literature (Extended Data Table 4a). In contrast to the RDD, however, areas with increased nightlight intensity are much more extensive than areas with high road density, so the URB alone marked about 3,900 river reaches as impacted, representing 1% of all impacted river reaches (Extended Data Fig. 5f).

It should be noted that in the final CSI calculations the individual pressure indicators can overlap or complement each other to reduce the CSI below the 95% threshold, hence the total number of impacted river reaches is not the sum of the individual values stated above, but all factors together impact a total of approximately 269,000 river reaches (Extended Data Table 4b). Given the cautious selection of the CSI threshold and weights, we believe that overall our conservative settings tend more towards under- than overestimation of the extent of impacted river reaches.

Sensitivity analysis. A thorough uncertainty analysis could not be performed at this point owing to the lack of information about the complex uncertainties of underpinning global datasets, such as erosion, water use, roads and urban areas. Instead, we conducted three basic sensitivity analyses to assess the robustness of our settings and findings.

First, we assessed the CSI distributions and boundaries by calculating the minimum, maximum, mean, range and standard deviation of the CSI values across all 100 scenarios for each individual river reach, and added these statistics to the final river reach dataset. We then averaged the individual standard deviations into bins of 5% CSI ranges (Extended Data Fig. 6a). We found that higher CSI ranges generally have lower standard deviations and that the standard deviations in the two bins around the chosen CSI threshold (95%) are below 4%, indicating that our results are robust around the CSI threshold that we chose to determine the free-flowing status of rivers.

Second, we calculated multiple iterations of scenario 11 with CSI thresholds varying from 80% to 100% (Extended Data Fig. 6b) to test the sensitivity of the CSI threshold setting. The results show that the agreement with benchmark FFRs is stable up to a CSI threshold of 95%, yet deteriorates quickly for higher CSI values. This finding indicates that a threshold setting above 95% (that is, triggered by very small fragmentation effects) is too strict and identifies too many rivers as non-free-flowing. By contrast, thresholds below 95% (triggered only by higher fragmentation effects) identify an increasing number of rivers as free-flowing, including all benchmark FFRs. This analysis corroborates our CSI threshold of 95% to be a meaningful setting, marking the transition spot between being too strict and too loose.

Third, as our understanding of the propagation of fragmentation impacts from dams in the upstream direction is particularly limited, we tested the importance of the upstream part of the DOF. We found that if upstream effects of the DOF were excluded, the CSI increased in about 25% of impacted river reaches, representing 2.2% of all analysed reaches globally. However, the number of rivers that regain FFR status amounts to only 1,468 (about 102,000 km) and is restrained mostly to short rivers. Nevertheless, we recommend that the parameters defining the magnitude and extent of the DOF index be further investigated.

Identification of FFRs. Using the backbone concept described in section 'Hydrographic framework' (Extended Data Fig. 2) and considering a CSI threshold of 95%, we classified the river network into:

1. FFRs: rivers that are above the CSI threshold from their source to the river outlet.

2. Good connectivity status: a river reach or a stretch of a river that is above the CSI threshold, but other river reaches or stretches of the same river are below the CSI threshold.

3. Impacted: any river reach, stretch or entire river that is below the CSI threshold.

In some cases, a major river may have a few river reaches or short stretches below the CSI threshold (for example, owing to a small fragmentation in a remote headwater location), which, according to our definitions, would render the entire river as non-free-flowing. To limit these minor artefacts, we excluded impacts of small reaches or stretches that affect less than 0.1% of the total flow of the river (in terms of average natural discharge). Globally, this filter only affects 431 river reaches or stretches with an approximate length of 1,800 km.

Data availability

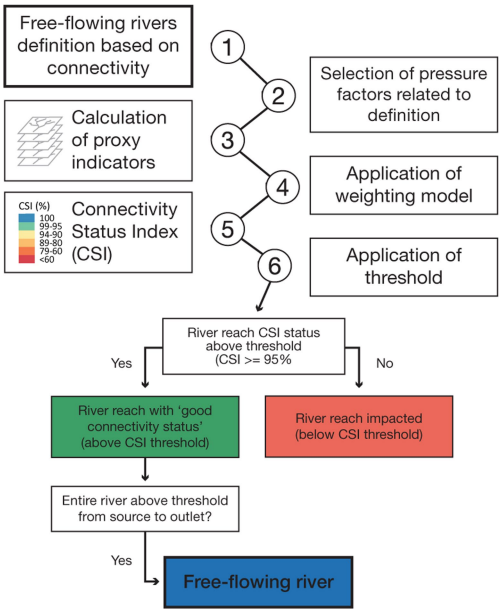
The geometric dataset of the global river network and the associated attribute information for every river reach—that is, the values of all pressure indicators (DOF, DOR, SED, USE, RDD and URB)—as well as the main results of the study—that is, values for the CSI, the dominant pressure factor and the FFR status— are available at https://doi.org/10.6084/m9.figshare.7688801 under a CC-BY-4.0 license. The dataset can be used together with the published source code (see 'Code availability') to recalculate the main study results and to run existing and new scenarios. The databases of dams required to calculate the DOF, DOR and SED indicators are not in the data repository owing to licensing issues, but are freely available at http://www.globaldamwatch.org. Original data that supported the study—that is, raw datasets of roads, urban areas, water use, waterfalls, erosion data and floodplain information—and their sources are summarized in Extended Data Table 1. Additional higher-resolution maps of Figs. 1–3 are available at http://www.hydrolab.io/ffr.

Code availability

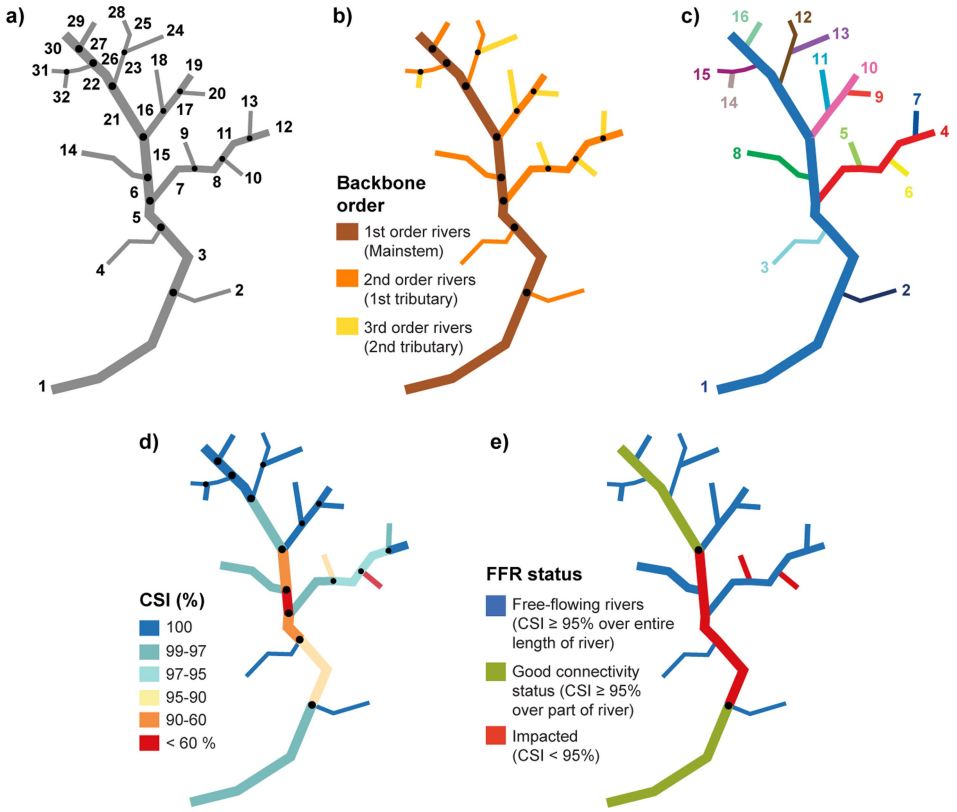
The source code of the main tools, scripts and algorithms used in this research is available under the GNU General Public License v3.0 at https://github.com/ggrill/Free-Flowing-Rivers. Other procedures and GIS steps (as described in Methods) were conducted manually and are therefore not part of the code repository.

51. WWF. *Free-Flowing Rivers: Economic Luxury or Ecological Necessity?* (WWF, Gland, 2006).
52. Döll, P., Kaspar, F. & Lehner, B. A global hydrological model for deriving water availability indicators: model tuning and validation. *J. Hydrol.* **270**, 105–134 (2003).
53. Alcamo, J. et al. Development and testing of the WaterGAP 2 global model of water use and availability. *Hydrol. Sci. J.* **48**, 317–337 (2003).
54. River discharge data. *Global Runoff Data Centre, Federal Institute of Hydrology, Koblenz, Germany* https://www.bafg.de/GRDC (2014).
55. Armstrong, J. S. in *Long-range Forecasting: From Crystal Ball to Computer* 2nd edn, 346–354 (Wiley, New York, 1985).
56. Kruk, A. & Penczak, T. Impoundment impact on populations of facultative riverine fish. *Ann. Limnol. Int. J. Lim.* **39**, 197–210 (2003).
57. Herbert, M. E. & Gelwick, F. P. Spatial variation of headwater fish assemblages explained by hydrologic variability and upstream effects of impoundment. *Copeia* **2003**, 273–284 (2003).
58. Ponton, D. & Copp, G. H. Early dry-season community structure and habitat use of young fish in tributaries of the River Sinnamary (French Guiana, South America) before and after hydrodam operation. *Environ. Biol. Fishes* **50**, 235–256 (1997).
59. Reyes-Gavilán, F., Garrido, R., Nicieza, A., Toledo, M. & Brana, F. Fish community variation along physical gradients in short streams of northern Spain and the disruptive effect of dams. *Hydrobiologia* **321**, 155–163 (1996).
60. Pracheil, B. M., McIntyre, P. B. & Lyons, J. D. Enhancing conservation of large-river biodiversity by accounting for tributaries. *Front. Ecol. Environ.* **11**, 124–128 (2013).
61. Messager, M. L., Lehner, B., Grill, G., Nedeva, I. & Schmitt, O. Estimating the volume and age of water stored in global lakes using a geo-statistical approach. *Nat. Commun.* **7**, 13603 (2016).
62. Lehner, B., Ariwi, J. & Grill, G. HydroFALLS: a global waterfall database. http://wp.geog.mcgill.ca/hydrolab/ (2016).
63. Dynesius, M. & Nilsson, C. Fragmentation and flow regulation of river systems in the northern third of the world. *Science* **266**, 753–762 (1994).
64. Constantine, J. A., Dunne, T., Ahmed, J., Legleiter, C. & Lazarus, E. D. Sediment supply as a driver of river meandering and floodplain evolution in the Amazon Basin. *Nat. Geosci.* **7**, 899–903 (2014).
65. Harvey, A. M. The influence of sediment supply on the channel morphology of upland streams: Howgill Fells, Northwest England. *Earth Surf. Process. Landf.* **16**, 675–684 (1991).
66. Vörösmarty, C. J. et al. Anthropogenic sediment retention: major global impact from registered river impoundments. *Global Planet. Change* **39**, 169–190 (2003).
67. Petts, G. E. & Gurnell, A. Dams and geomorphology: research progress and future directions. *Geomorphology* **71**, 27–47 (2005).
68. Schmitt, R. J. P., Rubin, Z. & Kondolf, G. M. Losing ground – scenarios of land loss as consequence of shifting sediment budgets in the Mekong Delta. *Geomorphology* **294**, 58–69 (2017).
69. Rubin, Z. K., Kondolf, G. M. & Carling, P. A. Anticipated geomorphic impacts from Mekong basin dam construction. *Int. J. River Basin Manage.* **13**, 105–121 (2015).
70. Latrubesse, E. M. et al. Damming the rivers of the Amazon basin. *Nature* **546**, 363–369 (2017).
71. Kondolf, G. M. et al. Changing sediment budget of the Mekong: cumulative threats and management strategies for a large river basin. *Sci. Total Environ.* **625**, 114–134 (2018).

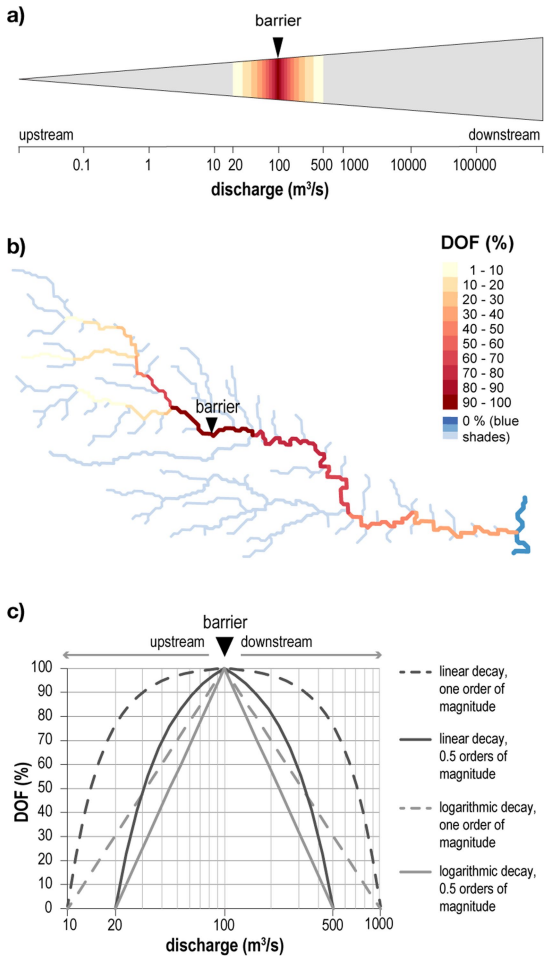
72. Turowski, J. M., Rickenmann, D. & Dadson, S. J. The partitioning of the total sediment load of a river into suspended load and bedload: a review of empirical data. *Sedimentology* **57**, 1126–1146 (2010).
73. Borrelli, P. et al. An assessment of the global impact of 21st century land use change on soil erosion. *Nat. Commun.* **8**, 2013 (2017).
74. Brune, G. M. Trap efficiency of reservoirs. *Trans. Am. Geophys. Union* **34**, 407 (1953).
75. Morris, G. L. & Fan, J. *Reservoir Sedimentation Handbook: Design and Management of Dams, Reservoirs, and Watersheds for Sustainable Use* (McGraw-Hill, New York, 1998).
76. Kummu, M., Lu, X. X., Wang, J. J. & Varis, O. Basin-wide sediment trapping efficiency of emerging reservoirs along the Mekong. *Geomorphology* **119**, 181–197 (2010).
77. Meybeck, M., Laroche, L., Dürr, H. H. & Syvitski, J. P. M. Global variability of daily total suspended solids and their fluxes in rivers. *Global Planet. Change* **39**, 65–93 (2003).
78. Milliman, J. D. & Farnsworth, K. L. *River Discharge to the Coastal Ocean: A Global Synthesis* (Cambridge Univ. Press, Cambridge, 2013).
79. Vanmaercke, M., Poesen, J., Broeckx, J. & Nyssen, J. Sediment yield in Africa. *Earth Sci. Rev.* **136**, 350–368 (2014).
80. Guo, L. C., Su, N., Zhu, C. Y. & He, Q. How have the river discharges and sediment loads changed in the Changjiang River basin downstream of the Three Gorges Dam? *J. Hydrol.* **560**, 259–274 (2018).
81. Yang, H. F. et al. Human impacts on sediment in the Yangtze River: a review and new perspectives. *Global Planet. Change* **162**, 8–17 (2018).
82. Wang, Y., Rhoads, B. L., Wang, D., Wu, J. & Zhang, X. Impacts of large dams on the complexity of suspended sediment dynamics in the Yangtze River. *J. Hydrol.* **558**, 184–195 (2018).
83. Dang, T. H. et al. Long-term monitoring (1960–2008) of the river-sediment transport in the Red River Watershed (Vietnam): temporal variability and dam-reservoir impact. *Sci. Total Environ.* **408**, 4654–4664 (2010).
84. Fan, H., He, D. & Wang, H. Environmental consequences of damming the mainstream Lancang–Mekong River: a review. *Earth Sci. Rev.* **146**, 77–91 (2015).
85. Fu, K. D., He, D. M. & Lu, X. X. Sedimentation in the Manwan reservoir in the Upper Mekong and its downstream impacts. *Quat. Int.* **186**, 91–99 (2008).
86. Meijer, J. R., Huijbregts, M. A. J., Schotten, K. C. G. J. & Schipper, A. M. Global patterns of current and future road infrastructure. *Environ. Res. Lett.* **13**, 064006 (2018).
87. Tessler, Z. D., Vorosmarty, C., Grossberg, M., Gladkova, I. & Aizenman, H. A global empirical typology of anthropogenic drivers of environmental change in deltas. *Sustain. Sci.* **11**, 525–537 (2016).
88. Wang, L., Lyons, J., Kanehl, P. & Bannerman, R. Impacts of urbanization on stream habitat and fish across multiple spatial scales. *Environ. Manage.* **28**, 255–266 (2001).
89. Booth, D. B. & Jackson, C. R. Urbanization of aquatic systems: degradation thresholds, stormwater detection, and the limits of mitigation. *J. Am. Water Resour. Assoc.* **33**, 1077–1090 (1997).
90. Grimm, N. B. et al. Global change and the ecology of cities. *Science* **319**, 756–760 (2008).
91. Doll, C. N. CIESIN thematic guide to night-time light remote sensing and its applications http://ngdc.noaa.gov/eog/dmsp/downloadV4composites.html#AXP (2008).
92. Henderson, J. V., Storeygard, A. & Weil, D. N. Measuring economic growth from outer space. *Am. Econ. Rev.* **102**, 994–1028 (2012).
93. Small, C., Pozzi, F. & Elvidge, C. D. Spatial analysis of global urban extent from DMSP-OLS night lights. *Remote Sens. Environ.* **96**, 277–291 (2005).
94. Schneider, A., Friedl, M. A. & Potere, D. A new map of global urban extent from MODIS satellite data. *Environ. Res. Lett.* **4**, 044003 (2009).
95. Fluet-Chouinard, E., Lehner, B., Rebelo, L. M., Papa, F. & Hamilton, S. K. Development of a global inundation map at high spatial resolution from topographic downscaling of coarse-scale remote sensing data. *Remote Sens. Environ.* **158**, 348–361 (2015).
96. Richter, B. D. et al. Lost in development's shadow: the downstream human consequences of dams. *Water Altern.* **3**, 14–42 (2010).
97. Nilsson, C. & Jansson, R. Floristic differences between riparian corridors of regulated and free-flowing boreal rivers. *Regul. Riv. Res. Manage.* **11**, 55–66 (1995).
98. Gupta, H., Kao, S.-J. & Dai, M. The role of mega dams in reducing sediment fluxes: a case study of large Asian rivers. *J. Hydrol.* **464–465**, 447–458 (2012).
99. Vörösmarty, C. J., Douglas, E. M., Green, P. A. & Revenga, C. Geospatial indicators of emerging water stress: an application to Africa. *Ambio* **34**, 230–236 (2005).
100. Smakhtin, V., Revenga, C. & Döll, P. A pilot global assessment of environmental water requirements and scarcity. *Water Int.* **29**, 307–317 (2004).
101. Pastor, A. V., Ludwig, F., Biemans, H., Hoff, H. & Kabat, P. Accounting for environmental flow requirements in global water assessments. *Hydrol. Earth Syst. Sci.* **18**, 5041–5059 (2014).
102. Brauman, K. A., Richter, B. D., Postel, S., Malsy, M. & Flörke, M. Water depletion: an improved metric for incorporating seasonal and dry-year water scarcity into water risk assessments. *Elem. Sci. Anth.* **4**, 000083 (2016).
103. Blanton, P. & Marcus, W. A. Railroads, roads and lateral disconnection in the river landscapes of the continental United States. *Geomorphology* **112**, 212–227 (2009).
104. Shuster, W. D., Bonta, J., Thurston, H., Warnemuende, E. & Smith, D. R. Impacts of impervious surface on watershed hydrology: a review. *Urban Water J.* **2**, 263–275 (2005).
105. Schueler, T. R., Fraley-McNeal, L. & Cappiella, K. Is impervious cover still important? Review of recent research. *J. Hydrol. Eng.* **14**, 309–315 (2009).



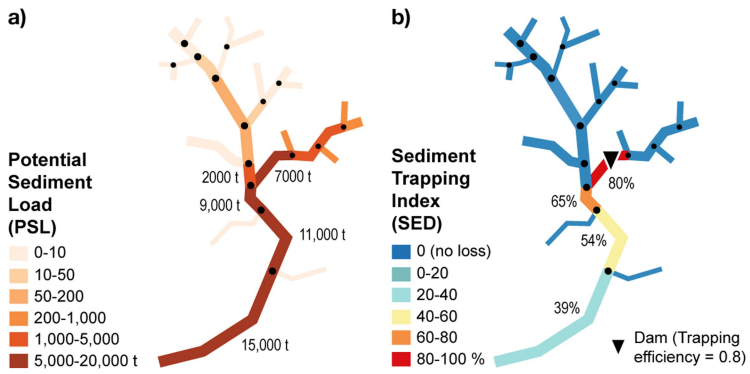
Extended Data Fig. 1 | Workflow for mapping FFRs. Methodological steps to define and assess the CSI of individual river reaches (steps 1–5) and decision tree used to assess the free-flowing status of entire rivers (step 6 and following).



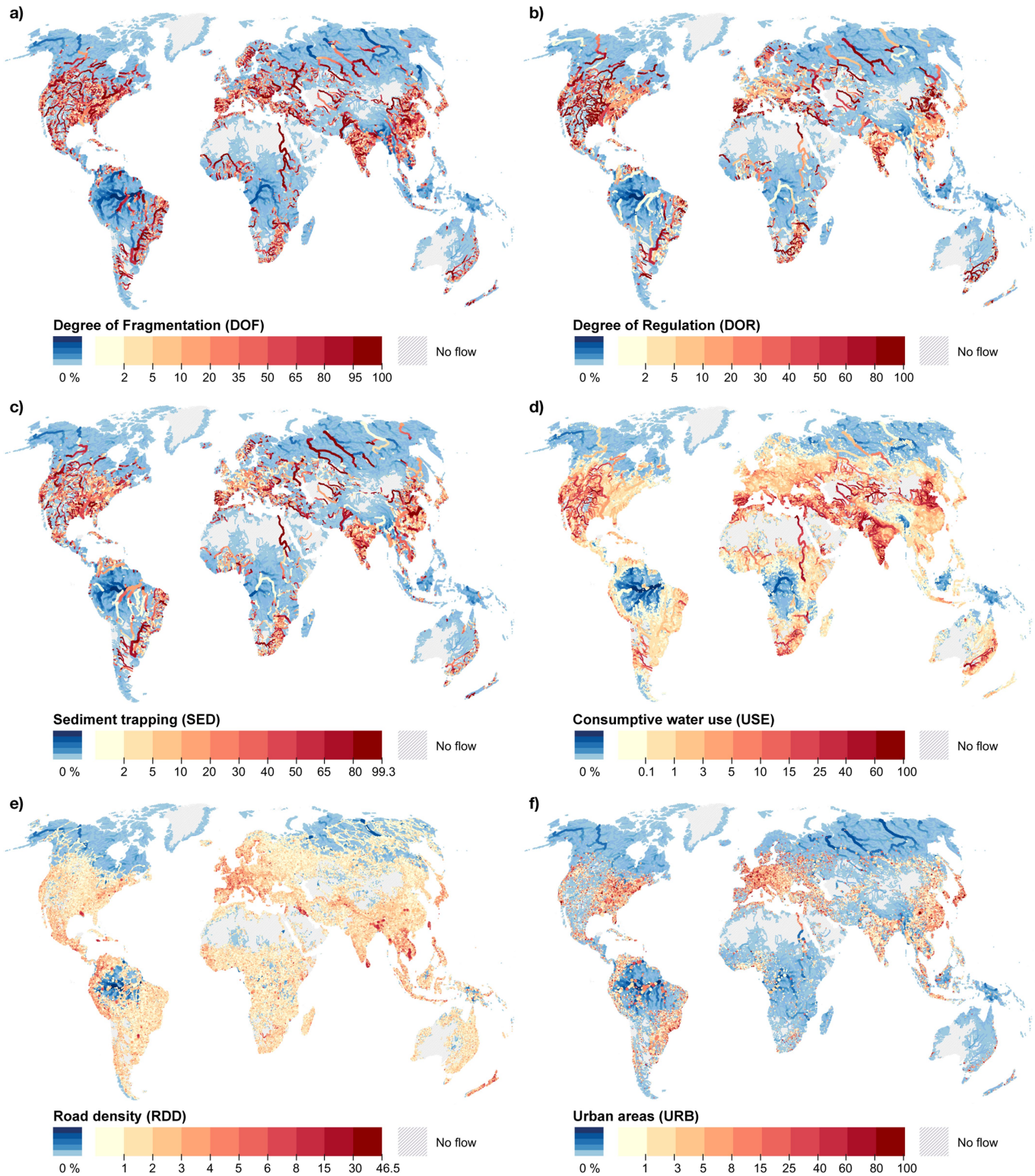
Extended Data Fig. 2 | Schematic overview of river-related concepts used in this study. a–c, The baseline river network consists of individual 'river reaches' (1–32 in **a**), defined as line segments separated by confluences (black dots). River reaches can be aggregated into 'rivers' according to a 'backbone' ordering system, which classifies river reaches as the mainstem or a tributary of various higher orders (**b**). Following this system, the river network can be distinguished into distinct rivers (1–16 in **c**), defined as contiguous stretches of river reaches from source to outlet on the mainstem or from source to confluence with the next-order river. **d**, CSI values for individual river reaches, as calculated with our model. If a value is at or above the CSI threshold (95%), the river reach is declared to have good connectivity status; if it is below the threshold, it is declared to be impacted. **e**, If an entire river (as defined in **c**) has good connectivity status, it is defined to be an FFR (blue). A river can be partly above the CSI threshold, and thus contiguous stretches can have good connectivity status (green).



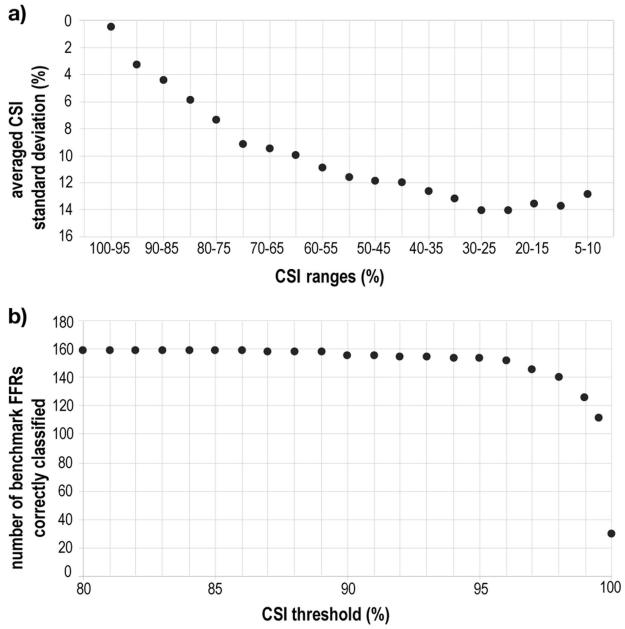
Extended Data Fig. 3 | Conceptual approach of DOF calculation, and visualization for a river example. a, **b**, The DOF index ranges from 0% (no fragmentation impact) to 100% (completely fragmented) and is shown for the conceptual approach (**a**) and the river example (**b**) in the colour coding shown in **b**. It is calculated for all river reaches connected to the barrier location in both the up- and downstream directions (but tributaries to the mainstem downstream of the barrier are not considered affected). The impact is largest in connected river reaches that are similar in discharge to the barrier site and diminishes as rivers become increasingly dissimilar in size, that is, larger in the downstream or smaller in the upstream direction. **c**, DOF decay functions, as considered and evaluated by the expert group.



Extended Data Fig. 4 | Schematic representation of the approach used to calculate the SED. The SED ranges from 0% to 100%, assessing the degree to which sediment connectivity in any river reach is altered by upstream dams. **a**, River network with individual river reaches and PSL ranges. **b**, The SED, which accounts for the relative contribution of tributaries to the total sediment budget of the river network, and its changes in response to changes in longitudinal sediment connectivity.



Extended Data Fig. 5 | Spatial distribution and magnitude of pressure indicators. a–f, Individual indicators within their range of occurrence, between 0% and 100%. The colour schemes are nonlinear and vary between indicators. The blue shades represent the magnitude of river discharge for river reaches with pressure values of 0% (that is, darker shades for larger rivers).



Extended Data Fig. 6 | Sensitivity analysis for CSI values and thresholds. a, Averaged CSI standard deviations for CSI ranges. **b**, Number of benchmark FFRs correctly classified at different CSI thresholds.

Extended Data Table 1 | Pressure factors and indicators used in this study

Pressure factor	Pressure indicator	Description	Connectivity aspect affected	Source data
River fragmentation	DOF	Degree of Fragmentation	Longitudinal	HydroSHEDS; Lehner et al.[31], GRanD v1.1; Lehner et al.[2], GOODD v1.0; Mulligan et al.[32], HydroFALLS; Lehner et al.[62]
Flow regulation	DOR	Degree of Regulation	Lateral, temporal	HydroSHEDS; Lehner et al.[31], GRanD v1.1; Lehner et al.[2], GOODD v1.0; Mulligan et al.[32], HydroLAKES; Messager et al.[61]
Sediment trapping	SED	Sediment trapping index	Longitudinal, lateral, vertical	Erosion map; Borrelli et al.[73], HydroSHEDS; Lehner et al.[31], GRanD v1.1; Lehner et al.[2], GOODD v1.0; Mulligan et al.[32], HydroLAKES; Messager et al.[61]
Water consumption	USE	Consumptive water use (abstracted from surface or groundwater)	Longitudinal, lateral, vertical, temporal	WaterGAP v2.2; Döll et al.[52], Alcamo et al.[53], HydroSHEDS; Lehner et al.[31]
	RDD	Road density	Lateral, longitudinal	GRIP v3; Meijer et al.[86], GIEMS-D15[95]
Infrastructure development in riparian and floodplain areas	URB	Nightlight intensity in urban areas	Lateral	DMSP-OLS v4; Doll[91], Urban areas; Schneider et al.[94], GIEMS-D15[95]

Overview of pressure factors, related pressure indicators and their relationship with connectivity aspects, as well as datasets and data sources required to calculate the pressure indicators.

Extended Data Table 2 | River stretches with good connectivity status

a)	'Good Connectivity Status' (number of stretches)				
	10–100 km	100–500 km	500–1000 km	>1000 km	Total
Africa	462	149	18	4	633
Asia	2428	302	24	8	2762
Australia	231	39	4		274
Europe	1339	290	15	2	1646
North America	1480	248	5	1	1734
South America	860	164	10	7	1041
Total	6800	1192	76	22	8090

b)	'Good Connectivity Status' (thousand km)				
	10–100 km	100–500 km	500–1000 km	>1000 km	Total
Africa	18.2	31.7	12.9	4.9	67.6
Asia	73.3	57.0	16.0	15.3	161.6
Australia	8.0	8.2	2.5	0.0	18.7
Europe	47.0	53.7	10.1	2.1	113.0
North America	52.1	44.7	2.7	1.0	100.6
South America	28.6	32.1	7.1	13.2	81.0
Total	227.2	227.3	51.4	36.1	542.4

Number (**a**) and length (**b**) of river stretches with good connectivity status (CSI $\geq$ 95%).

Extended Data Table 3 | Characteristics and results of selected scenarios

SCE	Weights (%)						Impacted reaches (< 95%)	Mean CSI	Benchmark rivers correct	Number of reaches predominantly affected by pressure indicator *						
No.	DOF	DOR	SED	USE	RDD	URB	%	%	%	DOF	DOR	SED	USE	RDD	URB	Total
11	30	30	15	15	5	5	9.3	93.3	96.9	185,218	63,356	11,300	7,477		1,899	269,250
20	35	25	15	15	5	5	9.3	93.0	96.9	212,472	36,232	10,986	7,505		1,893	269,088
33	35	25	15	10	10	5	9.2	93.1	96.9	212,538	36,454	11,175	4,002	2	1,823	265,994
37	30	30	15	10	10	5	9.2	93.3	96.9	185,429	63,543	11,514	3,998	6	1,827	266,317
43	20	15	5	50	5	5	9.4	95.2	97.5	189,994	26,758	745	53,772		2,311	273,580

Key statistics of the five best scenarios, including scenario weightings, impacted reaches (CSI < 95%), mean CSI and number of reaches where a pressure indicator is dominant, and percentage of correctly predicted benchmark FFRs (see Supplementary Table 3 for all 100 scenarios).
*Reaches are counted if the pressure indicator causes the strongest effect on the CSI index, taking into account multiple pressure indicators.

Extended Data Table 4 | Scenario weighting and corroboration

a) Overview of literature

Pressure indicator	Range of values reported (%)	Relevant literature and case studies
DOF	10-50	Pracheil et al.[60]; expert review; case studies in Tapajos, Luangwa and Upper Ganges River
DOR	2-15	Richter et al.[96]; Nilsson and Jansson[97]; Nilsson and Berggren[11]; Lehner et al.[2]
SED	> 30	Syvitski et al.[18]; Rubin et al.[69]; Vörösmarty et al.[66]; Gupta et al.[98]
USE	10-50	Vörösmarty et al.[99]; Smakhtin et al.[100]; Pastor et al.[101]; Brauman et al.[102]
RDD	5-30	Blanton and Marcus[103]; Shuster et al.[106]
URB	> 80 *	Booth and Jackson[91]; Blanton and Marcus[103]; Schueler et al.[105]; Shuster et al.[104]

b) Characteristics of selected scenario 11

Pressure indicator	DOF	DOR	SED	USE	RDD	URB	Sum
Weights (%)	30	30	15	15	5	5	100
SPL (95%)	16.7	16.7	33.3	33.3	100	100	n.a.
Number of river reaches predominantly affected by pressure indicator †	185,218	63,356	11,300	7,477	0	1,899	269,250
Number of river reaches affected by pressure indicator alone ‡	242,446	131,259	101,241	18,357	0	3,906	n.a.

a, Overview of literature used to corroborate the scenario weightings. **b**, Characteristics of selected weighting scenario. Scenario 11 was selected on the basis of benchmarking results, its SPL, as well as the corresponding weighting values[96–105].

*Index based on nightlights to represent urban effects, scaled.

†Reaches are counted if the pressure indicator causes the strongest effect on the CSI index, taking into account multiple pressure indicators.

‡Reaches are counted if the pressure indicator causes any effect on them.